Master Thesis

An experimental study on the Spray characteristics of Diesel and Ethanol using the Constant Volume Chamber under varied injection duration and pressure

The Graduate School

of the University of Ulsan

Department of Mechanical Engineering

Tran Quang Khai

An experimental study on the Spray characteristics of Diesel and Ethanol using the Constant Volume Chamber under varied injection duration and pressure

Supervisor: Ocktaeck Lim

A Thesis

Submitted to

The Graduate School of the University of Ulsan

In partial Fulfillment of the Requirements

For the Degree of

Master of Science

by

Tran Quang Khai

Department of Mechanical Engineering

Ulsan, Korea

June 2023

An experimental study on the Spray characteristics of Diesel and Ethanol using the Constant Volume Chamber under varied injection duration and pressure

This certifies that the thesis of Tran Quang Khai is approved

Committee Chair, Prof. Park, Kyu Yeol (박규열)

Committee Member, Prof. Lee, Yoon Ho (이윤호)

Committee Member, Prof. Lim, Ock Taeck (임옥택)

Department of Mechanical Engineering

Ulsan, Korea

June 2023

ACKNOWLEDGMENT

First and foremost, I would like to express my sincere gratitude to Prof. Ock-Taeck Lim for his enthusiasm and immense knowledge. Their guidance helped me in all the research and writing this thesis. I am really lucky to have had an opportunity to work as a their graduate.

I thank my fellow labmates in the Smart Powertrain Lab: Mr. Nguyen Ho Xuan Duy, Mr. Quach Nhu Y, and other lab members for enlightening me on the first glance of research, for supporting me in my daily life, for the stimulating discussions an,d for all the fun we have had in the last two years.

I also send my best gratitude to my beloved family who has always been by my side and support me during the time, and to my beloved life-friend, Miss. Ngoc Han for having the final touch to perfect my documentations.

Last but not the least, I also take this opportunity to express a deep sense of gratitude to all employees and professors at the Department of Mechanical Engineering, University of Ulsan for their wonderful work.

ABSTRACT

One of the alcohols that is considered as a possible additive to diesel fuel is ethanol. This is due, among other things, to the fact that this alcohol can be produced from raw materials of plant origin and therefore can be considered as a fully renewable fuel. It is also important that dehydrated ethanol exhibits a relatively good solubility in diesel fuel compared to its counterparts. Furthermore, ethanol (C_2H_5OH) is one of the most important components of biodiesel fuel and promising alternative fuel in IC engines. Oxygenates such as ethanol has been widely used in IC engines because of their improved volatility and higher latent heating properties. Nonetheless, there are some complications such as lowered heating value, phase separation, pour point and unsafety conditions for storage and transportation of the ternary blends. With this respect, a blending between Diesel and Ethanol for conduct of the experimental study on spray characteristics using a constant volume combustion chamber was carried out. In this thesis, a blending percentage of 20% ethanol at 99.9% purity and 80% diesel will be utilized, which is denoted as DE20. A single hole research injector is utilized to inject the fuel into the combustion chamber. Due to the optical access of the Constant Volume Chamber (CVC), the spray images of the injected fuel have been analyzed to determine the spray development, spray penetration length, spray cone angle, spray area and spray volume. On the other hand, as there is no moving piston in CVCC, a typical diesel engine-like condition prior to fuel injection has been generated by nitrogen insertion to desirable pressure under ambient temperature. Two different ambient density conditions of 15 and 30 kg/m^3 similar to CI engine condition is demonstrated with three different injection pressures. The common rail fuel injection pressure was maintained equally to investigate the low to high injection pressure range; 500 bar, 800 bar and 1100 bar respectively. At the same time, injection duration variations from 800 to 2000 μs with the step of 400 μs are also

considered with an aim to lay the scope on during which time the injector starts to partly open until reaching fully opened. Indeed, a test matrix has been created to demonstrate the experimental results. The results of the all-about spray characteristics will be illustrated, making it a useful reference for future spray analysis of new fuels. At the same time, this use of diesel-ethanol can open up new opportunity for the reduction in diesel consumption and reduce undesirable emissions.

Keywords: diesel-ethanol blends; spray characteristics; spray development; spray penetration length; spray cone angle; spray area; spray volume; constant volume chamber; shadowgraph technique.

TABLE OF CONTENTS

LIST OF FIGURES

LIST OF TABLES

LIST OF ABBREVIATIONS

CVCC	Constant Volume Combustion Chamber
CV	Constant Volume
ORE	Optical Research Engine
RCM	Rapid Compression Machine
CPFR	Constant Pressure Flow Rig
CVHC	Constant Volume Hot Cell
CVPC	Constant Volume Precombustion Chamber
GB00	Pure gasoline
B100	Pure biodiesel
GB05	blend of 5% biodiesel & 95% gasoline
GB10	blend of 10% biodiesel & 90% gasoline
GB20	blend of 20% biodiesel & 80% gasoline
GB40	blend of 40% biodiesel & 60% gasoline
PCCI	Premixed charge compression ignition
GCI	Gasoline Compression Ignition
N2	Nitrogen gas
EGR	Exhaust gas recirculation
PTFE	Polytetrafluoroethylene
PID	proportional –integral –derivative

B5	5% biodiesel and 95% petroleum diesel blend
ICE	Internal Combustion Engine
O2	Oxygen gas
NOx	Nitrous oxide
CO	Carbon mono oxide
HC	Hydrocarbon
CI	Compression Ignition
CO2	Carbon dioxide
PM	Particulate matter
HD	Heavy duty
DPF	Diesel Particulate Filter
LNT	Lean NOx Trap
SCR	Selective Catalytic Reduction
LTC	Low-temperature combustion
HCCI	Homogeneous charge compression ignition
PPCI	Partially premixed compression ignition
CN	Cetane Number
HHV	Higher heating value
LHV	Lower heating value

1. INTRODUCTION

1.1 Background

Combustion research is a key pathway to further enhance the knowledge of combustion processes and injection of fuel. The better understanding will motivate researchers to find out the critical parameter to optimize next generation high-efficient low emission engine.

Optimization of these processes for more efficient combustion and reduced emission levels is directly dependent on the experimental approach and scientific understanding of spray and combustion phenomenology in this field. Research on combustion processes and injection has a very small-time domain and is highly dependent on the thermodynamic state of the environment; ambient pressure, density, temperature and other factors related to air fuel mixture and geometry of the combustion chamber. For simulating and visualizing engines like in-cylinder condition without any compression and expansion strokes, several types of combustion rigs are utilized. Among them, rapid compression machine, constant pressure flow rig, constant volume hot cell, constant volume pressure cell and optical research engines have been used in numerous research institutes with different research strategies. [1,2]. Figure 1 compares different experimental test rigs according to the experimental operating range in terms of temperature, pressure, and density where the description of experimental simulation approach is provided in **Table 1.1** [3]. **Figure 1**.1 compares the operating condition and area for various test rigs to simulate CI engine's in-cylinder conditions prior to fuel injection. Among different optical test rigs e.g. ORE1 [4], ORE2 [5], RCM [6], CPFR [7], CVHC [8] and CVPC [9] covers the full range in **Figure 1.1**.

Table 1.**1** describes a basic experimental methodology for the different test rigs, while **Table 1.2** compares the weaknesses and strengths of the different spray and combustion test rigs facility [3]. In this respect, CVPC, CPFR, and CVHC are found the best suited optical test rigs for the core research on free spray development and spray combustion.

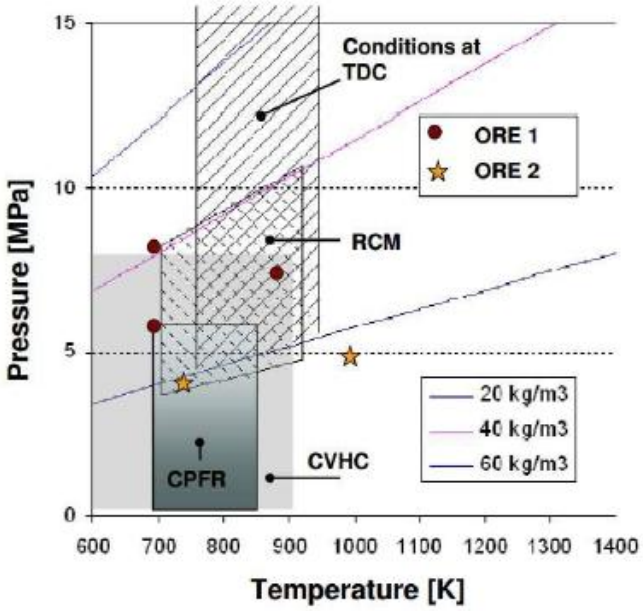

Table 1.1 Experimental approaches to obtain in-cylinder condition of different test rig [3]

Test rig	Acronym	Simulates
Optical Research Engine	ORE	These engines have optical access into the combustion chamber
Constant Volume Hot Cell	CVHC	Chamber increases the temperature with external heat elements.
Constant Volume Pressure Cell	CVPC	Chamber using pre-combustion technique to press urize the rig to simulate the TDC conditions right before fuel injection.
Rapid Compression Machine	RCM	One compression stroke during an engine cycle
Constant Pressure Flow Rig	CPFR	Chamber using additional flow into the rig to pres surize the rig

The constant volume combustion chamber (CVCC) of Smart Powertrain Lab at University of Ulsan is a Constant Volume Pressure Cell (CVPC) in accordance with Table 1.1. The term CVCC and CVPC will be used interchangeably in this thesis. This CVCC is previously used to conduct an experimental investigation on non-reactive and non-vaporizing fuel spray of different types of alternative fuel using either multi-hole or single hole fuel injector with a pressurized common rail system.

Table 1.2 Quality attributes of different optical spray test facility (mostly relative; 0= neutral, + better, - worse)

Type of optical test rig	ORE	RCM	CPFR	CVHC	CVPC
Optical accessibility	0	0	++	-	+
Similarity to the real engine situation	0	-	--	--	--
Free spray penetration distance	0	+	+++	++	++
Control on trapped gas p / T	0	+	++	++	++
Control on trapped gas composition (i.e. EGR)	0	-	+	++	+++
Flow field impact on combustion	--	-(-)	0	-	-
Test facility volume	0	+	0	++	++
Time to switch between test conditions (i.e. T)	0	0	0	--	++
Time between tests [s]	1	120-600	1-3	60	600

Figure 1.1 Non-reactive fuel spray in inert atmosphere using multi-hole fuel injector

Figure 1.2 Non-reactive fuel spray in inert atmosphere using single hole fuel injector

The non-reactive and non-vaporizing sprays are studied when the CVCC is either filled with the inert N_2 gas, see **Figure 1.2** and **Figure 1.3** respectively. On the other hand, reactive, vaporizing spray and spray combustion can be investigated when the chamber is prepared for precombustion, e.g. an oxidizer is present inside the heated and pressurized CVCC.

1.2 Aims and Objectives

This master thesis focuses on the investigation of the fuel spray and combustion characteristics of gasoline biodiesel blended fuel using a constant volume combustion

chamber. Each blended fuel results will be compared to observe a best possible alternative fuel in this study. The objectives are given below:

1. Carrying out a literature review on global energy demand, renewable energy and ethanol as well as its blended fuel
- Introducing the topic of renewable energy & biofuel;
- Describing relevant fuel spray and combustion characteristics:
- Describing the test equipment and the experimental methodology.
2. Preparing and assembling the combustion chamber for visualization of the spray characteristics of injected fuels
3. Performing fuel spray visualization test in the combustion chamber
- Testing fuel according to the matrix and test procedure;
- Performing non-vaporizing experiment;
- Performing experiment using appropriate imaging technique.
4. Analyzing the experimental result
- Analyzing image to obtain the spray penetration length, cone angle, area, and volume;
- Calculating statistical evaluation of the data.

1.3 Motivation

The motivation of this study is to examine the potentiality of gasoline biodiesel blended fuel for future compression ignition engines. A better understanding of most effective alternative liquid fuel spray and combustion characteristics is crucial for improving fuel economy and determining the appropriate air-fuel mixture to diminish exhaust emission of direct injected compression ignition engine. Experiments are conducted using an optical accessible Constant Volume Combustion Chamber (CVCC) which helps to visualize the spray and combustion formation inside the CVCC. Nitrogen is utilized during the non-vaporizing spray experiment to generate the desired ambient gas density condition similar to the equivalent load at the compression stroke in compression ignition engine. On the other hand, combustion characteristics are investigated by using the precombustion techniques to generate the high-pressure high-temperature condition. These images along with the acquired pressure trace data are analyzed in this study. Usually, canola oil, corn oil, used cooking oil and animal fats are employed to formulate the biodiesel. However, the major percentage of the biodiesel is prepared from the soybean oil. Biodiesel is advantageous due

to its renewable characteristics which can be mixed with traditional diesel fuel to prepare a fuel blend. All the modern diesel-based transportations can use up to 5 percent biodiesel (B5) blend with conventional diesel fuel. Currently, the demand for diesel as a transportation fuel is much higher than gasoline while the source of fossil fuels is limited. The utilization of gasoline biodiesel fuel blend in compression ignition engine can improve the efficiency and emission while the demand for the diesel fuel can be decreased. As a result, pure gasoline and four different gasoline-biodiesel blended fuels will be tested and then investigate to determine the spray and combustion characteristics retrieved from the fuel spray image and experimental data set. The spray characteristics indicate the result of spray tip penetration, spray cone angle, spray area and spray volume. The combustion characteristics contain the result of ignition delay which is obtained from the rate of heat release. The blended gasoline biodiesel fuels will be injected at three different fuel injection pressures at two different ambient gas density with appropriate imaging techniques. The images will be used to determine the spray characteristics while the acquired pressure data will be used to determine the combustion characteristics e.g. the ignition delay.

1.4 Thesis outline

Chapter 1 illustrates why this master thesis is inscribed, give a brief introduction to the topic of the thesis and to put it in context with preceding studies done on the same issue. The improvements are briefly described with the research aims and objective.

Chapter 2 briefly explains the current energy situation and future energy demand for the targeted emission legislation. Internal emission formation in CI engine and emission standard are summarized to propel high efficiency low emission CI engine architecture in future.

Chapter 3 describes alternative energy and biofuels. This chapter has been included to give the thesis a broader perspective, to highlight the importance of alternative fuel to the reader for a deeper understanding of the core mechanisms driving research in this field.

Chapter 4 describes the experimental equipment, the working principles, subsystems, limitations of this research and optical imaging techniques used to obtain the raw data. The fuels sprays are depicted in more detail in the result section where the comparison is taken for different fuel at different condition.

Chapter 5 deals how the experimental test and analysis procedures are conducted and the essential characteristics where fuel spray, air fuel interaction, spray and spray combustion characteristics are explained. This chapter presents the theory behind and serves as the fundament for understanding, the different characteristics which make up the basis for comparison in this study.

Chapter 6 aims to explain the result and discussion from the experimental test for the experimental environment such as non-vaporizing test condition where the spray penetration, cone angle and volume is measured. For the spray combustion test the ignition delay and heat release is analyzed in more detail.

Chapter 7 contains the conclusion as well as some concluding remarks and suggestions to further work. Throughout this thesis, some equations are rewritten with appropriate reference to clear how to calculate different parameters. All the used symbols are listed under the symbols section.

2. Future Fuel Demands and Emission Impacts to the Environment

2.1 Global Energy Forecast

As the world population grows and economies expand, energy demand is expected to continue increasing. However, there is growing recognition of the need to transition to a more sustainable energy system that reduces greenhouse gas emissions and mitigates the impacts of climate change. By looking at trends and analyzing data from 2021 and beyond, we can make some predictions about the future of energy.

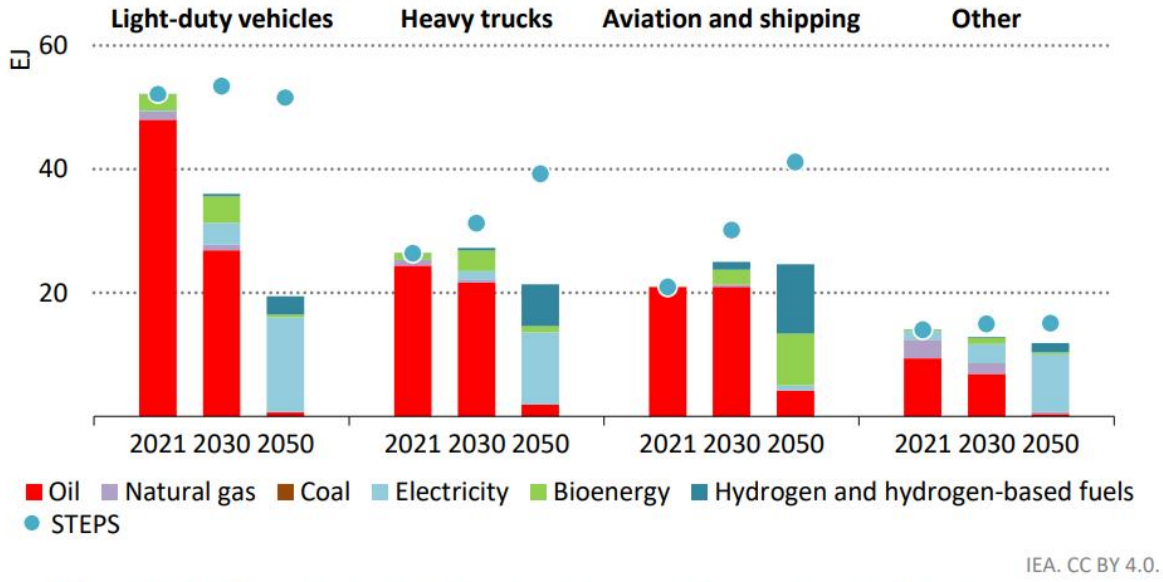

Figure 2.1 Final energy consumption in transport by source and mode in the NZE Scenario, 2021-2050

One of the most significant trends we have seen in recent years is the continued growth of renewable energy. According to the International Energy Agency (IEA), renewable energy sources are set to account for 90% of the global power capacity added in 2021 and 2022. Wind and solar energy are the fastest-growing sources of renewable energy, and their costs have continued to decline. The IEA has projected that renewables will account for nearly 70% of the global electricity mix by 2040. This trend is driven by a combination of factors, including declining costs, policy support, and growing public awareness of the need to reduce greenhouse gas emissions.

While renewable energy is expected to grow rapidly, fossil fuels are not going away anytime soon. According to the IEA, global demand for coal is set to rise in 2021 and 2022, after declining in 2019 and 2020 due to the COVID-19 pandemic. Natural gas is also expected to continue to play a significant role in the energy mix, particularly in power generation. However, there is growing recognition of the need to reduce greenhouse gas emissions from fossil fuels. This has led to a shift towards cleaner-burning natural gas and the development of technologies such as carbon capture and storage.

Another important trend in the future of energy is the increasing focus on energy efficiency. According to the IEA, energy efficiency improvements could meet around half of the global emissions reduction targets set out in the Paris Agreement. Improvements in energy efficiency can be achieved through a combination of technology, policy, and behavior change. Transportation: The transportation sector is also undergoing significant changes, driven by a combination of technological innovation and policy support.

Electric vehicles (EVs) are becoming increasingly popular, and the IEA has projected that EV sales could reach 145 million by 2030. This would require significant investment in charging infrastructure and battery technology. In addition to EVs, there is growing interest in alternative fuels such as hydrogen and biofuels. However, these technologies are still in the early stages of development and face significant challenges in terms of cost and scalability.

Overall, the future of energy is likely to be characterized by a transition to a more sustainable and diverse energy mix. Renewable energy will play an increasingly important role, while fossil fuels will continue to be used but in a cleaner and more efficient way. The transportation sector will undergo significant changes, driven by the growth of electric and alternative fuel vehicles. Energy efficiency improvements will also play a key role in reducing greenhouse gas emissions. While the transition to a more sustainable energy system will not be easy, there are many reasons to be optimistic about the future of energy.

Renewable energy sources, such as wind, solar, hydroelectric, and geothermal, are rapidly becoming the backbone of the energy mix in many countries. In addition to these sources, biofuels, such as ethanol and biodiesel, are also gaining popularity as a way to reduce greenhouse gas emissions from transportation. In this article, we will explore ethanol and other related biofuels in more detail.

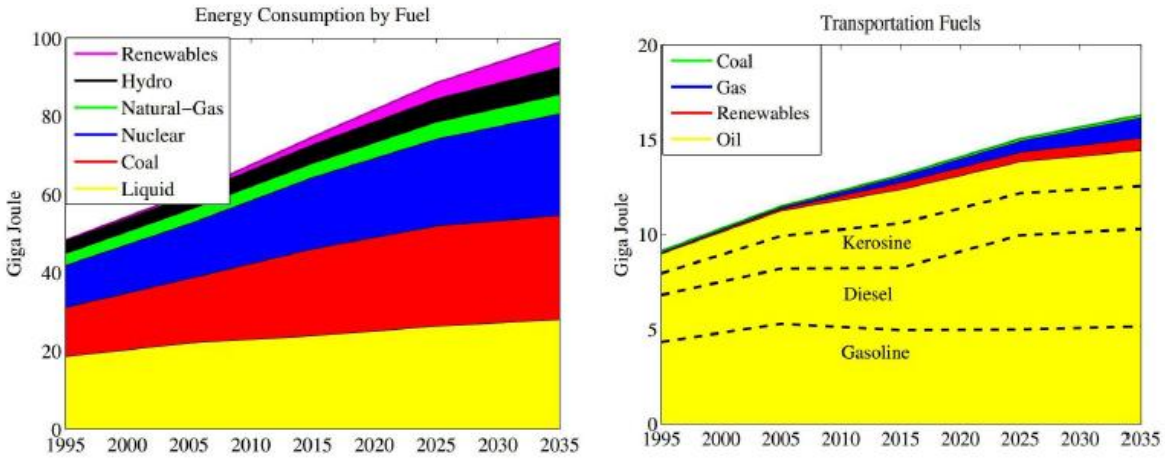

Figure 2. 2 Predicted future energy consumption by fuel (left) and the predicted energy source diversification for the transportations fuel (right). Data retrieved from [10,13]

Predictions of short and long-term fuel based energy consumption are depicted in **Figure 2.2** where each of the fuels has shown a potential increase in upcoming future. The primary reason behind this predicted increase is the continuous growing global population, starting from 6.8 billion in 2014 to 8.6 billion in 2035 [10]. The second reason is all the B.R.I.C. countries (Brazil, Russia, India and China) are equally advanced in newly economic development [11]. This development will directly lead to an increased local usage of transportation that results in higher energy consumption [12]. The compression ignition combustion engine is still the most important power sources for the heavy duty, railway, marine transport, agricultural machinery and stationary applications (referred as medium speed diesel engines)[13]. The shrinking crude oil resources, increasing energy demand, strict emission regulations and concern about the environment (e.g. greenhouse effect) are the main motivations behind searching alternative fuels and energy conversion methods. According to the European directive 2003/30/EG, 25% of the fuel used by the road transport should be renewable fuel by 2030.

Ethanol is a biofuel made from fermenting and distilling corn, sugarcane, or other plant material. It is often blended with gasoline to produce a fuel known as E10, which contains up to 10% ethanol, or E85, which contains up to 85% ethanol. Ethanol is a renewable fuel that produces fewer greenhouse gas emissions than gasoline. In recent years, ethanol production has increased significantly, particularly in the United States and Brazil. In the United States, ethanol production has risen from 1.6 billion gallons in 2000 to over 15 billion gallons in 2021. Brazil is the world's largest producer of ethanol, and more than 60% of the

country's transportation fuel comes from ethanol.

Biodiesel is another type of biofuel made from vegetable oils, animal fats, or recycled cooking grease. It is often blended with diesel fuel to produce a fuel known as B20, which contains up to 20% biodiesel. Biodiesel production has also increased in recent years, particularly in Europe and the United States. According to the European Biodiesel Board, biodiesel production in the European Union increased from 4.8 million tonnes in 2010 to 12.3 million tonnes in 2021. In the United States, biodiesel production has increased from 750 million gallons in 2010 to over 2.5 billion gallons in 2021.

In addition to ethanol and biodiesel, there are many other types of biofuels being developed and tested around the world. For example, cellulosic ethanol is made from non-food crops such as switchgrass, corn stover, and forestry residues. Algae-based biofuels are also being researched as a potential source of renewable fuel.

Despite the potential of biofuels to reduce greenhouse gas emissions from transportation, there are also challenges to their widespread adoption. One of the biggest challenges is the availability of feedstocks. Ethanol is often made from corn, which is a food crop, and there are concerns that using food crops for fuel could lead to higher food prices and land use conflicts. Biodiesel is often made from vegetable oils, which can also compete with food production. Another challenge is the cost of production. While the cost of biofuels has declined in recent years, they are still more expensive to produce than fossil fuels. This can make them less competitive in the marketplace, particularly when oil prices are low. Conclusion: Despite the challenges, biofuels such as ethanol and biodiesel have the potential to play an important role in reducing greenhouse gas emissions from transportation. As technology continues to improve and costs continue to decline, biofuels could become an increasingly important part of the energy mix. However, it will be important to carefully manage the production of biofuels to ensure that they are sustainable and do not compete with food production.

2.2 CI Engine Emission

A wide range of emissions is generated due to the heterogeneous combustion in the

engine cylinder that usually releases in the atmosphere through the tailpipe of the exhaust stream. While considering the engine exhaust, other emissions of the engine such as heat, and sound are not accountable. The major gaseous emissions from the CI engine are:

Nitrogen Oxides (NO_x) Nitrogen from the air is oxidized during the combustion process to form nitrogen oxides. Fuel-bound nitrogen plays a minimal role. The N_2 and O_2 react with the equilibrium concentration of the NO_x compounds at around 2000K-3000K [14]. Nitrogen oxide is the predominant oxide of nitrogen formed during combustion with subsequent oxidation forming the NO_2. The NO_x formation is highly dependent on temperature through the so-called Zeldovich mechanism along with the duration of combustion and the local oxygen concentration [15]. NO_x is primarily formed on the lean portion of the diffusion combustion region where high temperatures help to raise the local equivalence ratio approximately 1 with higher oxygen concentration [16,17].

Carbon Monoxide (CO) A lack of oxygen concentration during combustion results in a higher concentration of CO. The main influence on CO emissions is, therefore, the air/fuel ratio. As with HC, the heterogeneous nature of the mixture can lead to locally fuel rich zones which will produce higher CO concentrations. At first, post-oxidation occurs which reduces the concentration of the mixture. CI engines usually run with excess air, operating within the low smoke limit. Hence CO emissions in CI engines are not normally significant.

Unburnt Hydrocarbons (HC) Incomplete combustion are typically responsible for the heterogeneous nature of the fuel-air mixture and the range of equivalence ratio. This exhaust gas carries a mixture of hydrocarbons into the stream.

In a CI engine exhaust stream, the mixture of HC compounds forms a broad range of molecular size. All of the HC emission will not exist in the gaseous phase.

Carbon Dioxide CO_2 is considered as one of the primary causes of anthropogenic climate change, a result of the complete oxidation of the carbon in the hydrocarbon fuel. The main non-gaseous emission of concern is soot. Soot is not a visibly defined substance, but in general terms, soot is a solid content consisting around eight parts carbon and one part hydrogen [18]. Soot in a CI engine is a product of pyrolysis or incomplete combustion of hydrocarbons which nucleates from the vapor phase to a solid phase in the locally fuel rich region of the reaction zone [18]. The generation of soot particles in a spray flame is characteristically a chemically-controlled phenomenon in which a particular portion of the

thermodynamic state is difficult to describe [19]. The oxidation of the primary particles will be a function of available oxygen, temperature, residence time and structure of the primary particle. Soot oxidation and formation is a highly complex sequence of reactions with the number of precursors and subspecies determining what is ultimately emitted in the engine's exhaust stream. Particulate matter (PM) is the amalgamation of soot and other liquid substances or solid phase materials contained in the exhaust flow. PM is often segregated into a soluble and an insoluble portion, with soot making up the insoluble portion. The fraction of PM which is typically soot, is often estimated by determining the insoluble part of the particulate and is generally higher than 50%. Other particulate matter constituents include: partially burned fuel/lubricant oil, bound water, wear metals and fuel-derived sulfate [18].

2.3. Strengthened Exhaust Regulation

The first noticeable point in the transportation sector is increasing energy consumption and second significant part is the exhaust gas emissions which has attracted much attention in recent days. All kind of vehicles are facing more stringent emission regulation as a major air pollution sources in the urban and rural roads. The main exhaust gases are nitrogen oxides (NO_x), carbon monoxide (CO), unburned hydrocarbon (HC) and soot/ particle matters (PM) which have a strong odor. Those exhaust emitted gases and the pungent smell gases lead to seriously pollute the total atmosphere in cities. At the same manner, huge amounts of carbon dioxide (CO_2) has been exhausted by IC engines will eventually lead the environment towards the greenhouse effect. As a result, the current generation and the upcoming generation will face a serious global warming and climate change. The general awareness of global warming and greenhouse gas effect have driven cities and countries to produce more and more stringent vehicle emission policy, especially for the diesel-fueled vehicles, while the understanding of the long-term health effects of emitted particles from vehicles on the human lungs is driving IC vehicles to become environmentally competitive with zero emission power drives from electric and fuel cell engines. Most of the developed countries have already schemed exhaust gas regulations to further limit the tailpipe emissions of the automotive vehicles. The primary emission regulation was entitled as ‘Euro 1’ settled by the Europe Union (EU) in 1992. During the last 20 years, the European emission regulations have been modified numerous times. Currently, the Euro VI scheme is followed by most of the countries which have become more and more stringent that the previously settled

regulation. The comprehensive EU emission regulations for HD diesel engines from the 'Euro 1' stage to the 'Euro 6' stage is plotted in **Figure 2.3**.

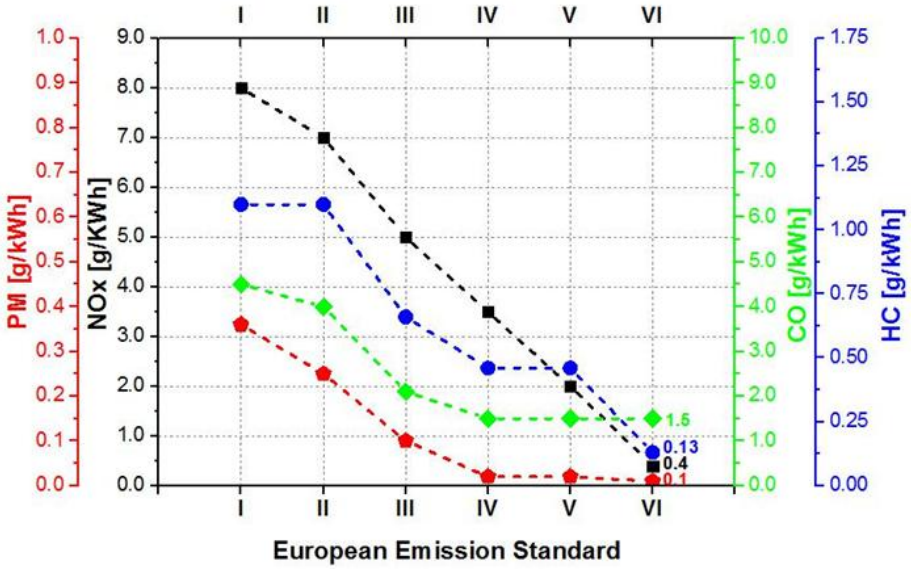

Figure 2.3 European emission regulations for passenger cars

Compared to the traditional gasoline engines, the emissions standard is more challenging for medium duty and heavy diesel engines. Usually, gasoline engines emit NO_x, CO and THC and emissions which can be eliminate by using a cost-effective three-way catalyst where the engine exhaust PM level is relatively low. The cost of modern days diesel engine technology has largely been driven by the emissions standard. The unveiling of Euro 5 standard has pushed all the diesel engine based automotive manufacturers to add an expensive Diesel Particle Filter (DPF). The current Euro 6 has been forcefully implemented the costly Lean NO_x Trap (LNT) or Selective Catalytic Reduction (SCR) system in a diesel engine. From the evolution of Euro I to Euro VI, the supplementary cost for a gasoline engine is negligible because the three-way catalyst has been utilized in the gasoline engine can handle most of the toxic emissions without any addition exhaust emission control equipment. However, the fitting of a SCR and DFP is fulfilling the requirement to meet EURO 6 which require more than double the total cost of emission control equipment. These oxidizer devices usually require noble metals or dangerous chemicals (e.g. ammonia in selective catalytic reduction) as catalyzer which also increases the vehicle manufacturing cost.

3. ALTERNATIVE ENERGY, ETHANOL AND ETHANOL-DIESEL BLENDING AS A FUEL

Blending ethanol with diesel fuel has been found to offer various benefits for the environment and public health. One of the significant advantages is the decrease in harmful emissions from diesel engines, as ethanol's higher oxygen content promotes more complete combustion and reduces particulate matter emissions. This reduction is crucial because particulate matter can lead to severe health effects, such as heart disease and respiratory problems. Additionally, blending ethanol with diesel can lower nitrogen oxide emissions, which contribute to air pollution and smog. Another benefit is the potential to enhance engine efficiency by producing more energy per unit of fuel and leading to improved fuel economy, hence reducing greenhouse gas emissions. In this study, ethanol diesel fuel blend with single injection methodology will be investigated.

3.1. Why is Ethanol of special interests?

The main objective of the research and development activities related to alternative fuels is to find fuels that are environmentally friendly and cost-competitive, with respect to petroleum-based fuels. In the short term, this means creating fuel blends based on diesel oil, while increasing the proportional content of bio-components, in order to produce “clean” fuels in the medium- and long-term without the use of petroleum products.

Esters from vegetable oils have been added to diesel fuel for decades, whereas recently, more attention has been paid to alcohols applied as fuel additives [20–22]. This may be linked to numerous favorable factors, such as high oxygen content and purity, as well as low viscosity [23,24]. The alcohols commonly used as alternative fuels include ethanol and methanol, which are products of biomass fermentation [25]. Used in mixtures with diesel oil, ethanol presents better properties than methanol [26]. The former more effectively blends into diesel oil and has a higher cetane number and superior lower calorific value [27].

Ethanol is the most commonly used alcohol because it can be obtained from a variety of raw materials [28] and at a low production cost [29]. Ethanol (C_3HCH_2OH) is a clear colorless liquid also known as ethyl alcohol, grain alcohol and EtOH. It is obtained through fermentation of biomass like corn, sugar beet, sugar cane and wheat (also called first generation ethanol). In order to obtain the desired purity, distillation is followed by a

dehydration process [30] [31] [32]. Currently, the largest ethanol producers in the world are Brazil and the USA (see Fig. 3.1 and 3.2 [30][34]).

Ethanol can be used as fuel for internal combustion engines either directly or in blends [34]. Making ethanol available as a vehicle fuel involves several steps:

• growth, collection and transportation of feedstock;

• production of first/second generation ethanol;

• preparation of E10, E15 or E85 and their distribution to the gas stations.

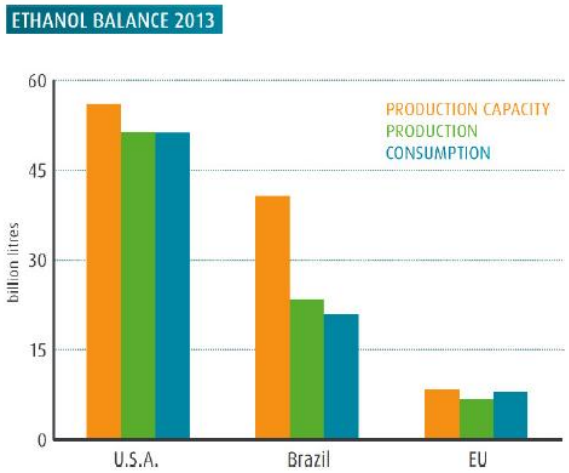

Figure 3.1 Ethanol production/consumption balance in 2013 [34]

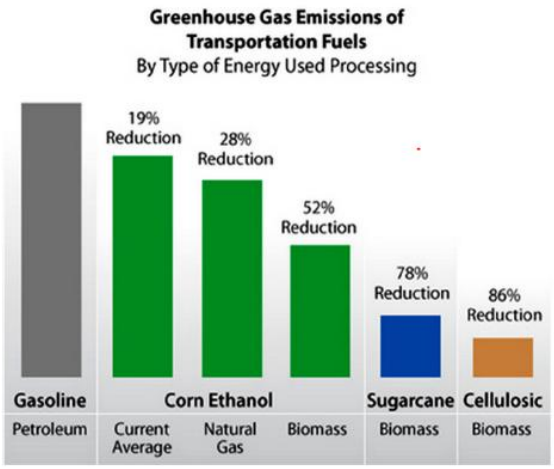

Figure 3.2 Greenhouse gas emissions of transportation fuels [30]

However, due to its low cetane number and lubricity, ethanol cannot be used as a stand-alone fuel to power compression ignition engines [35]. For this reason, mixing ethanol with diesel oil is a good solution [36,37]. The resulting blends can be used in compression ignition engines designed to run on conventional diesel fuel [38]. This subject matter has been investigated in numerous studies that have focused on various aspects related to the use of such fuel blends [39-41].

3.2. Ethanol blending with autoignition-based fuels

The idea of Diesel-ethanol blends is not new. Research studies dating since the 1980s have shown that these blends are suitable for use in compression ignition (CI) engines [42], [43], [44]. Pollutant emissions improvements associated with the use of DE blends in CI engines (without any modifications) are strongly dependent on the operating conditions of

the respective engine. By adjusting the injection parameters, this dependence could be controlled, and the benefits enhanced [45]. Diesel and ethanol have considerable different physical and chemical properties, which affect the properties of the resulting blend. A comparison between the main characteristics of ethanol and Diesel can be seen in **Table 3.1**:

Table 3.1 Main properties of Diesel and Ethanol [46][47][48], EN 590

Property	Fuel	
	Diesel	Ethanol (anhydrous)
Density at 15°C [kg/m^3]	820 - 845	792
Cetane number (CFR)	min. 51	~8
Lower Heating Value [MJ/kg]	43.700	26.900
Kinematic viscosity at 40°C [mm^2/s]	2 – 4.5	1.13
Flash point [°C]	min. 55	12.8
Autoignition temperature [°C]	~ 315	~ 423
C [wt. %]	~ 85.24	~ 52.17
H [wt. %]	~ 13.92	~ 13.04
O [wt. %]	~ 0.74	~ 34.78
S [wt. %]	max. 0.01	0.0
C/H mass ratio [-]	6.12	3.97
Stoichiometric Air/Fuel ratio [-]	14.60	9.01
Adiabatic flame temperature [°C] (determined from stoichiometric mixture at 9 MPa and 626 °C) [32]	2465	2401

3.2.1. Blend stability

The solubility of ethanol in Diesel fuel is affected mainly by two factors: environmental temperature and water content of the blend [29], [35]. At temperatures above 30°C, percentages of up to 15% v/v anhydrous ethanol can be mixed with Diesel without phase separation. However, at temperatures below 10°C and without the use of additives a phase separation can be observed. Another factor that can affect blend stability is the aromatic content of Diesel fuel, which acts, to some degree, as a bridging agent and co-solvent [49]. The water content of the blend affects not only the blend stability but also the combustion characteristics and the durability of the fuel injection system components [50]. Moreover, special measures must be taken when storing DE blends for longer periods because of an increased hygroscopic characteristic of ethanol. Due to variations in homogeneity of DE blends, a precise control of the injected ethanol quantity can be difficult and injection and combustion problems may arise. In order to stabilize the blend two methods are proposed: • addition of an emulsifier – it suspends small droplets of ethanol within Diesel fuel; • addition of a co-solvent – acts as a bridging agent between molecules [51]. Emulsification usually involves a series of heating and blending steps, whereas the use of co-solvents simplifies the

process by allowing "splash-blending" [29]. Some of the additives found by researchers ([51] [52] [53] [54] [55]) to inhibit phase separation are presented in **Table 3.2**:

Table 3.2 Identified additives for Diesel-ethanol stability

Additive	Observations
Tetrahydrofuran (THF)	Obtained from agricultural waste material
Ethyl acetate	Can be obtained from ethanol
PEC additive	Pure Energy Corporation of New York
AAE additive	AAE Technologies of the United Kingdom
GE Betz additive	Division of General Electrics
Biodiesel	Increases the percentage of biofuel in the blend

The required additive percentage is dictated by the lower temperature at which the blend stability must be guaranteed [52].

3.2.2. Cetane number

The cetane number of ethanol is estimated to have a value of 8, which is significantly lower than the minimum value of 51 imposed by EN 590 for Diesel. The cetane number is a measure of the fuels autoignition quality and dictates the ignition delay. This has a considerable influence on the fuel conversion efficiency, smoke emissions, noise, smoothness of operation and starting ease. Low values of the cetane number result in longer ignition delay, violent/incomplete combustion, reduced power output and a poor fuel conversion efficiency [53].

Adding ethanol to Diesel increases ignition delay and subsequently the rate of heat release (ROHR) but it leads to an improved brake thermal efficiency (BTE) of the engine. However, some adjustments to the injection strategy and timing could further improve the emission performances of the engine. Test performed by Moses et al. [54] showed some differences in the cetane number between DE emulsions and stable blends of aqueous ethanol and Diesel (without additive). They concluded that the ethanol emulsion had a lower influence on the cetane number of the blend. In order to improve the ignition qualities of DE blends, researchers have used cetane improvers like: 2EHN ([55] [56]), isooctyl nitrate ([57]), isoamyl nitrate ([58] [59]) etc.

3.2.3. Density

The density of a DE blend decreases proportionally with the ethanol content and/or temperature. Tests conducted by Torres-Jimenez et al. [39] showed that the density value of

a mixture containing 15% v/v ethanol remains within the standard reference limits. A decrease in density leads to a retarded start of injection, which can deteriorate the engines emission performances [11] but this problem can be solved by adjusting the injection timing [60]. Furthermore, for high pressure differences (injection pressure – cylinder pressure > 55 MPa), density is the only fuel property influencing the injector mass flow rate [61]. Therefore, a reduction of the injection density can lead to loss in engine power.

3.2.4. Viscosity

At 40°C, ethanol has a viscosity of about 1.1 mm^2/s, a value much lower than that of Diesel (2-4.5 mm^2/s) and therefore, it will lead to lower viscosity values of the blend. Still, according to the tests performed by Torres-Jimenez et al. [11] the viscosity value of a blend containing 15% v/v ethanol remained above the minimum value (2 mm^2/s) specified by the EN 590 standard [39]. A low viscosity value has negative influences on lubricity and on the maximum fuel delivery rate of the pump (due to the increased leakage). Ultimately, this results in a reduced power output of the engine. According to the study performed by Dernotte et al. [62], viscosity is also the main influencing parameter of the injector discharge coefficient when the difference between the injection pressure and the cylinder pressure is smaller than 55 MPa. The author noted an increase of the discharge coefficient when using a fuel with lower viscosity. However, a lower viscosity value has a positive influence on spray atomization: the mean Sauter diameter of the droplets is smaller and, as a consequence, the total surface area of the droplets increases; this facilitates the evaporation process.

3.2.5. Lubricity, corrosiveness, and engine wear

In order to protect the moving parts with which it comes in contact (by reducing the friction between solid surfaces in relative motion) the fuel must have a minimum level of lubricity. There are three ways used to evaluate fuel lubricity: vehicle testing (high fuel, time and effort demand), fuel injection bench test (is the most accurate) and laboratory lubricity tests (HFRR – High-Frequency Reciprocating Rig, SLBOCLE – Scuffing Load Ball-on-Cylinder Lubricity Evaluator). Diesel injection systems rely solely on the lubricating qualities of Diesel fuel. When mixing ethanol with Diesel, the resulting blend will have a lower lubricity than that of pure Diesel [63]. In spite of this reduction, a study performed by Lapuerta et al. [63] on a high frequency reciprocating rig at different temperatures, revealed that ethanol addition can in fact improve lubricity at high temperatures (60°C). This is

considered an effect of ethanol evaporation, which would compensate for its poorer tribological properties. Corrosiveness to copper tests performed by several authors [64] [65] revealed that ethanol addition does not lead to a higher corrosiveness than that of pure Diesel. Tested samples containing 5, 10 and 15% v/v of ethanol were classified as 1a [11]. EN 590 specifies for Diesel a class 1 corrosiveness to copper. Some early studies ([29] [66] [31] [30]) regarding engine wear when using DE blends (containing 10, 15 or 30% v/v anhydrous ethanol) have indicated no abnormal wear in the tested engines (the injection timing of the engines was adapted to the new fuel). A 500 h lab test with DE15 stabilized with PEC additive (2.35% v/v) on a Cummins ISB 235 engine reported no abnormal deterioration in engine condition [67]. In 2001, a test conducted on farm tractors using DE10 stabilized with GE Betz additive also reported, based on oil analysis, no abnormal wear of the engines [39]. Tests performed by Armas et al. [50] on two identical common rail injection systems revealed similar wear patterns of the fuel injection pump parts both for Diesel and the DE blend (7.7% v/v). However, an analysis of the injector nozzle showed a reduction of the nozzle section effective area, which lead to a decrease of the total fuel delivery by approximately 30%. This was believed to be a result of sedimentation/oxidation due to the increase in water content of the DE blend from 243 ppm (at the beginning of the test) to 640 ppm at the end of the 600 hours of testing. One other test, that studied the effect of ethanol addition to a diesel-biodiesel blend (7.7% v/v) on a common rail injection system, revealed similar wear patterns for both blends [68].

3.2.6. Low temperature operability

Several factors describe a fuels low temperature operability (or low temperature filterability), which is dependent not only on the presence of wax crystals but also on their shape and size. The standard test in Europe is the Cold Filter Plugging Point (CFPP) test, which requires the cooling of the fuel sample by immersion in a constant temperature bath (40°C/hour cooling rate). The CFPP is the temperature at which 20mL of fuel fail to pass through a wire mesh (45 Sm cell size and at 20 kPa vacuum pressure) in less than 60 s. Adding ethanol to Diesel does not significantly influence the value of the CFPP (Fig. 5). However, other properties like the cloud point, the plugging point and the filter plugging tendency show significant differences between DE blends and pure Diesel [11].

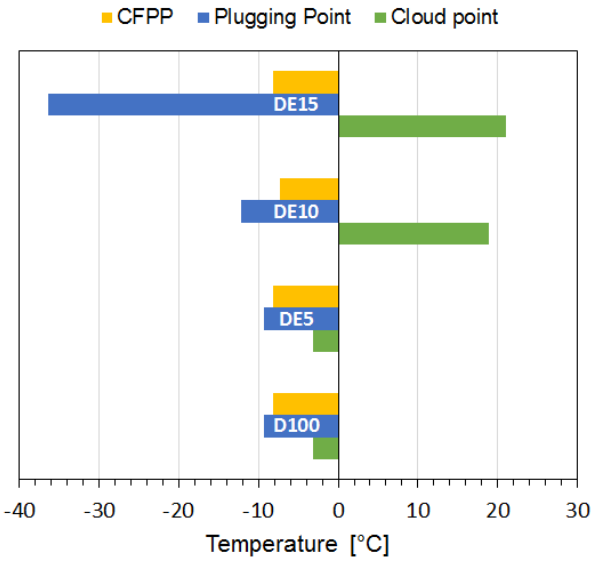

Figure 3.3 CFPP, CP, and PP of different Diesel-ethanol blends (after [11])

The cloud point (CP) is the temperature at which a cloud of was crystals first appears in a liquid when cooled under controlled conditions described in a standardized test. As can be seen in **Figure 3.3**, the addition of ethanol to Diesel fuel results in CP values much higher than that of pure Diesel and DE5 thus, highlighting the temperature dependence of DE blends. The plugging point (PP) is defined as the temperature at which fuel can no longer flow due to gel formation. The PP is improved but, for a content of 15% v/v ethanol the apparatus used by Torres-Jimenez et al. [39] displayed (due to phase separation) the ethanol PP and not the PP of the blend. For a precise determination of the PP, the blends need to be stable, that is, no phase separation can occur. In order to assess the tendency of particulates to plug or block the filter (which the CFPP cannot detect) the socalled Filter Plugging Tendency (FPT) value is calculated. Values determined by Torres-Jimenez et al. [39] showed a reduction in FTP and pumping pressure values proportional to the content of ethanol in the blend.

3.2.7. Distillation curve

The distillation curve is a fundamental fuel property, which shows the evaporation characteristics of a fuel [49]. It is used to calculate the cetane index and to evaluate the percentage of light, medium and heavy fractions, which are needed to characterize the fuels behavior during storage, at cold start, consumption characteristics and volatility. The initial boiling point of DE blends has a similar value as the boiling point of pure ethanol and, as a result, in the first part of the distillation curve, there is a considerable difference between the curve of the tested blends and that of pure Diesel (**Figure 3.4**). After the evaporation of the ethanol fraction, the distillation curves follow an almost identical trend [11]. When assessing

the environmental impact of a fuel, another important issue is biodegradability. Tests performed by Speidel et al. [59], [60] showed that fuels containing a higher degree of components derived from renewable sources are more degradable than conventional fossil fuels. The authors reported a 70% increase in biodegradability for DE blends as compared to pure Diesel.

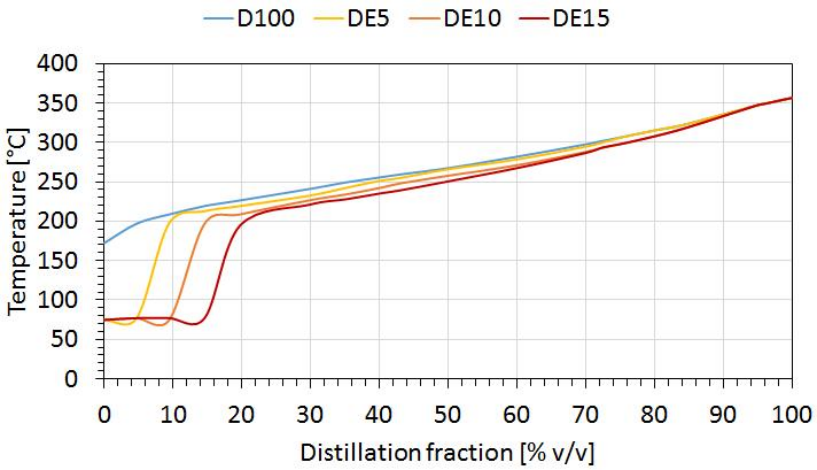

Figure 3.4 Distillation curves of Diesel and different Diesel-ethanol blends [11]

3.3. Ethanol blends' previous investigations

A study of the available literature on the topic of DE blends and their use in Diesel has led to the formulation of several conclusions, based on the majority of the reported findings:

I. Comparing the results of the reviewed literature revealed conflicting conclusions regarding the use of DE blends in Diesel engines. This is attributed to the considerable differences in the equipment and methodology used for testing;

II. Significant variations can be observed in the quantity of blended ethanol (with values ranging from 2% to 50% v/v) and in the fuel used as reference (Diesel, Diesel No. 2, Ultra-Low Sulfur Diesel and Low Sulfur Diesel);

III. There is a lack of papers covering the computer simulation of Diesel engines running on DE blends. When coupled with experiments, this is believed to be a more reliable way of investigation;

IV. Using DE blends leads to an increased ignition delay, which, in spite of

promoting mixture formation, can have negative effects on pollutant emissions. The retarded ignition timing is a result of the higher heat of vaporization value of ethanol and of its lower CN. As can be seen from the distillation curves (Fig. 5) the ethanol fraction evaporates before the Diesel fraction. This reduces the temperature in the combustion chamber and consequently increases the evaporation duration of Diesel. The extent of this influence is dependent on several engine construction factors and load. Adjustments of the injection timing or the use of cetane improvers can eliminate the possible inconveniences.

V. Due to the lower energy content of the resulting blend (proportional to the added ethanol percentage), a decrease in engine brake power is to be expected.

VI. When maintaining the same engine performances the brake specific fuel consumption (BSFC) increases along with the brake thermal efficiency.

VII. Low load tests revealed a decrease of smoke, PM and NOx emissions but an increase in CO and HC emissions. Due to the lower temperatures in the combustion chamber NO_x formation is inhibited but, this also affects the oxidation of CO to CO_2. The reduced smoke and PM emissions can be attributed to the reduced carbon content and, in the same time, to the increase the oxygen fraction contained in the fuel. During the increased ignition delay a higher amount of fuel is injected, which affects the mixture formation thus leading to increased HC emissions [40].

VIII. High load tests however, revealed a reduction of not only smoke, PM and NO_x but also of CO. The increased temperature promotes the oxidation of CO but is still lower than that of Diesel and thereby, leading to lower NOx emissions. Although having considerably lower values, HC emissions values remained above those of pure Diesel.

4. EXPERIMENTAL SETUP AND TESTING EQUIPMENT

4.1. Constant Volume Chamber Components

CVCC is a handy tool when studying the combustion properties of different fuels and can also be used to examine different types of fuel injector and spark plug technologies. The use of a CVCC in combustion research provides the possibilities to isolate the injection and combustion processes from all the influential subprocesses happening in an engine. The optical access makes it possible to see inside of the combustion chamber and this facilitates the use of a high-speed camera and the implementation of the image analyzing tools to achieve a better understanding of the injection and the combustion processes. The Smart Powertrain Lab's CVCC is cubically shaped with an internal volume of of 1.3 L (with all side solid) and 1.5 L (two side quartz and others side solid) respectively. Optical access is obtained by quartz windows of 200 mm diameter and 26 mm thickness. At this moment, the combustion vessel is optically accessible from two sides. To protect the glass and for safety purposes, a relief valve has been placed in the chamber. This limits the chamber maximum pressure up to 120 bar. No more higher pressures can be obtained over 100 bar due to the safety purpose. Inside the combustion chamber, an equipment is placed to obtain data from an experiment. The equipment is mounted in the vertical and horizontal section from the different side of the vessel as shown in figure 5.2. The magnetic driven mixing fan is employed to achieve a homogeneous mixture during the filling of the different gasses and a uniform temperature distribution during the pre-combustion. This is discussed in details in the next section of this chapter. Spark plug is used to ignite the gas mixture, thus initiating the pre-combustion. A fuel injector is placed in the combustion chamber in such a way that the injected fuel will propagate along the vertical axis of the chamber. This allows the fuel to travel the longest possible way before impinging to the opposite chamber wall.

In a real engine, successive combustion cycles will heat up the cylinder walls, affecting the internal processes. For this reason all the chamber walls can be heated up to 110°C by using the heater cartinge directly mounted in the chamber walls. Heating up the chamber walls is also employed to avoid the condensation of the quartz windows after pre combustion.

Smart Powertrain Lab's constant volume combustion chamber (CVCC) has been

modified to ensure the full control of different types of equipment at the same time domain. In the current modification, intake and exhaust valves can automatically and directly control from the LabVIEW program. A control box ensures the homogeneous mixing of the combustible gas by using a magnetically driven stirrer. Sprak plug can now initiate the spark ignition automatically after a given time duration in milisecond and the spark duration can be able to adjust by the user in microsecond scale. After the desired thermodynamic condition, fuel is injected for a very a short time frame and NI DAQ assistant records the value from the beginning of the precombustion until to a certain time after completing the spray combustion.

A picture and a schematic drawing of the experimental test facility are shown in **figures 4.1** and **4.2**. As it can be seen from the cut-through schematic, the CVCC is a cube-shaped vessel which has a large optically accessible combustion chamber of 110 mm from different sides, allowing extensive visualization of the fuel spray prior to wall impingement. For example, top window can be used for mixing fan and turbulence generation by using a rotating fan. Besides that, there are inlet and exhaust valves to deliver and vent gas in and out of the chamber, respectively. A dynamic pressure transducer (Kisler 6001) was placed in the bottom corner of the combustion vessel with pressure range of 0 to 250 bar. The combustion vessel is truly one of the kind experimental apparatus to understand the physics of combustion (spark-ignition or spray combustion) inside the vessel. Main chamber dimensions, sensors and acquisition apparatus are collected in **Table 4.1**.

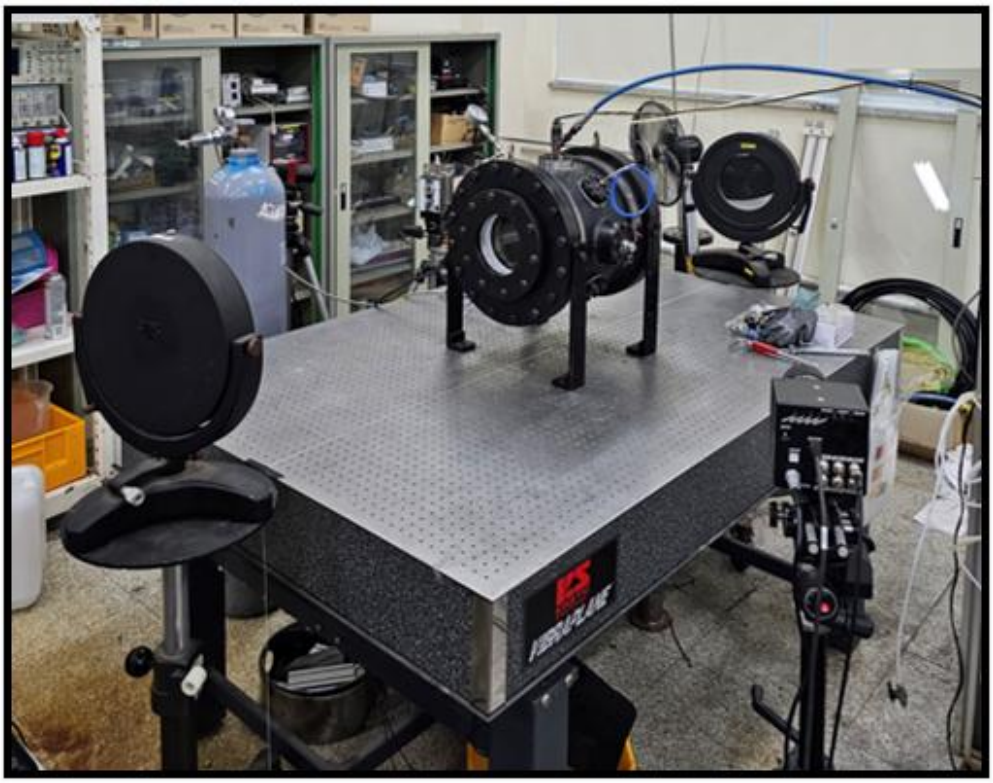

Figure 4.1 Pictorial layout of the experimental testbench

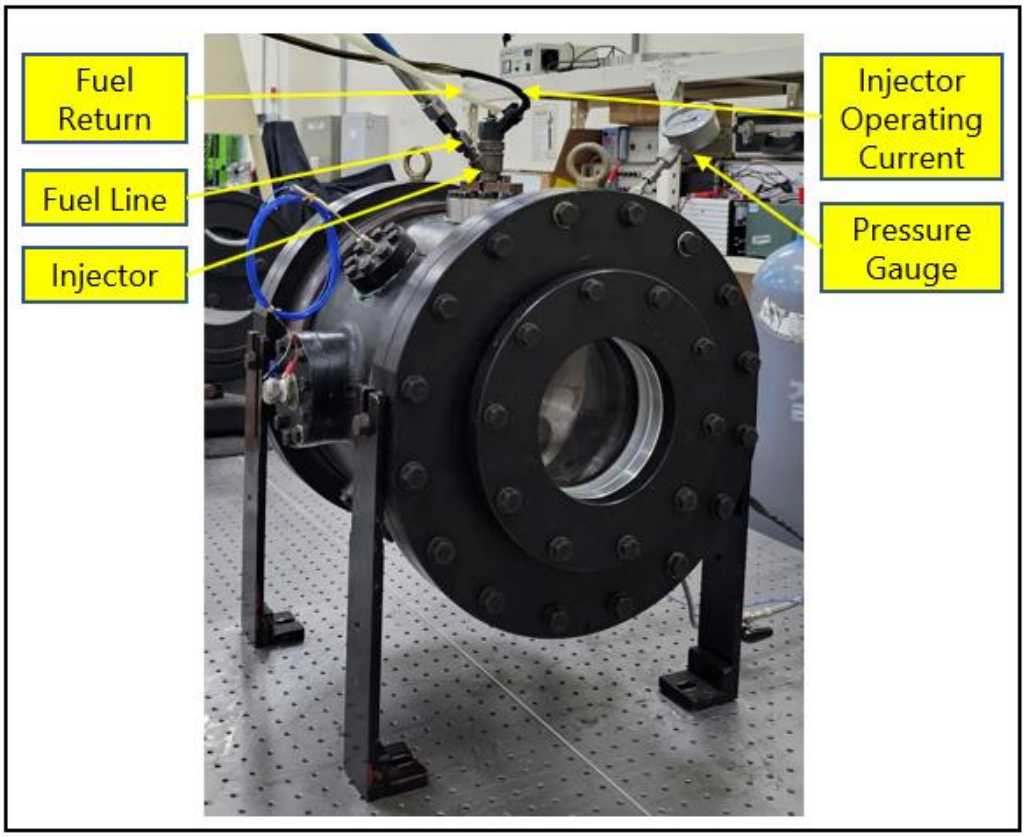

Figure 4.2 Assembled Constant Volume Chamber

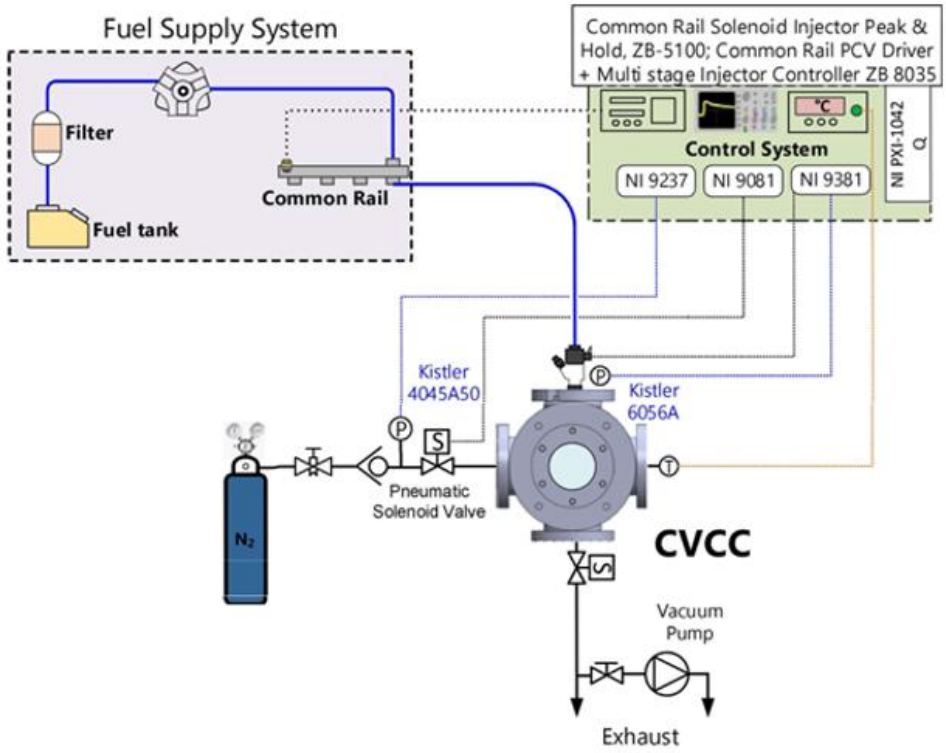

Figure 4.3 Schematic diagram of the test bench

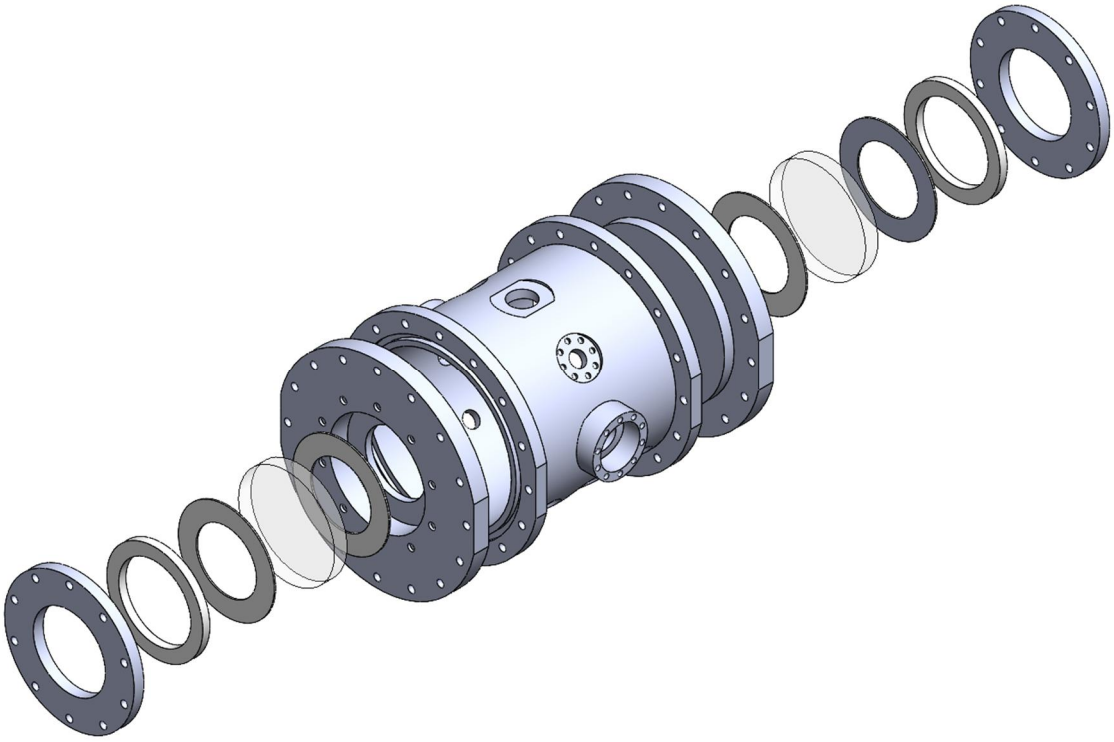

Figure 4.4 Exploded view of the Constant Volume Chamber

Table 4.1 An overall information of the test system and additional equipment

Basic Parameter		Unit
Shape of the internal chamber	115 × 115 × 115	mm
Window aperture	200	mm
Injector mounting	Upper Window	

Measurement Condition

	Minimum	Maximum	Unit
Ambient density	15	30	bar
Ambient temperature	298	298	K
Oxygen concentration	0	0.21	vol fraction
Wall temperature	293	293	K
Fuel temperature	Ambient	NA	K
Common rail pressure	500	1100	bar
Injection duration	800	2000	μs

Auxiliary system		
Proportional valve	Burkert 2875(only N 2), Burkert 2873	0-25, 0-16 bar
Ignition coils driver	Mobiq Ignition Coil Driver	

Sensor & Data Acquisition		
DAQ & control software	NI PXI 1042Q & LabVIEW	
Static gas pressure sensor	Peizo resistive Kristler 4045A50	0 - 50 bar
High Pressure calibrator	Sensys PSHHC020BCPG	0- 20 bar
Low pressure calibrator	Sensys PSHHC002BCPG	0- 2 bar
Dynamic gas pressure sensor	Peizo resistive Kristler 6056A	0 -250 bar
Vessel temperature sensor	Thermocouple K type **mm	
Module for Pressure measuement	NI927	
Module for Proportional Valve	NI928	

4.2. Subsystem

4.2.1 Common Rail Fuel System

Table 4.2 shows the key parameters of the fuel system. The fuel system is equipped with fuel lines capable of handling the properties of biofuel. The injector used in this study is a medium speed injector and it is fitted with a single hole injection nozzle with an orifice diameter of 33 mm. Between the tests of different fuels, the fuel system is completely emptied and fuel filter is cleaned appropriately. To make sure that all of the old fuel is flushed out of the system, the first couple of thousand injections after a fuel change are done in a

canister and this fuel is removed before the the start of testing.

Table 4.2 Common rail operating condition

Fuel pump operating condition	**Value**	**Unit**
Maximum pump pressure	0	Bar
Maximum pump pressure	1200	Bar
Maximum piping pressure	2500	Bar
Fuel temperature condition	Ambient	K

4.2.2 Control System

A computer is installed with the Photron Fastcam Viewer 4 (PFV4) to control the high-speed camera and to adjust all the camera setting before recording the pictorial strings with varied conditions. The injection signal is used for triggering of the high-speed camera recording.

4.3. Subsystem

4.3.1 Load condition

The most important and governing factor in the CVCC is the maximum pressure allowance. The peak pressure occurs during the pre-combustion, and is directly linked to the amount of energy we introduce to the CVCC in terms of composition of the gas mixture. The maximum vessel pressure of the CVCC is limiting the simulated load condition due to the rapid pressure increases during pre-combustion. The load condition is related to the charge air density, which in the CVCC, since the volume is constant, is represented by the density of the gas mixture. If the amount of gas that the CVCC is filled with is increased to simulate a higher load conditions, the risk overshooting the design pressure of the vessel during precombustion. Figure 15 shows a typical load condition curve for a medium speed one stage turbocharged CI engine. A break mean effective pressure (BMEP) of 50 bars corresponds to engine idling and at this load condition, the charge air density is 16.8 kg/m^3 at time of injection. Due to the rapid pressure increase during pre-combustion, the density limitation of the CVCC is 20 kg/m^3 and this corresponds to middle of low to medium load operation. The rapid pressure increase can be reduced by igniting a leaner gas mixture, but the current ignition system is not able to do that and work on finding a more powerful

ignition system is currently being conducted.

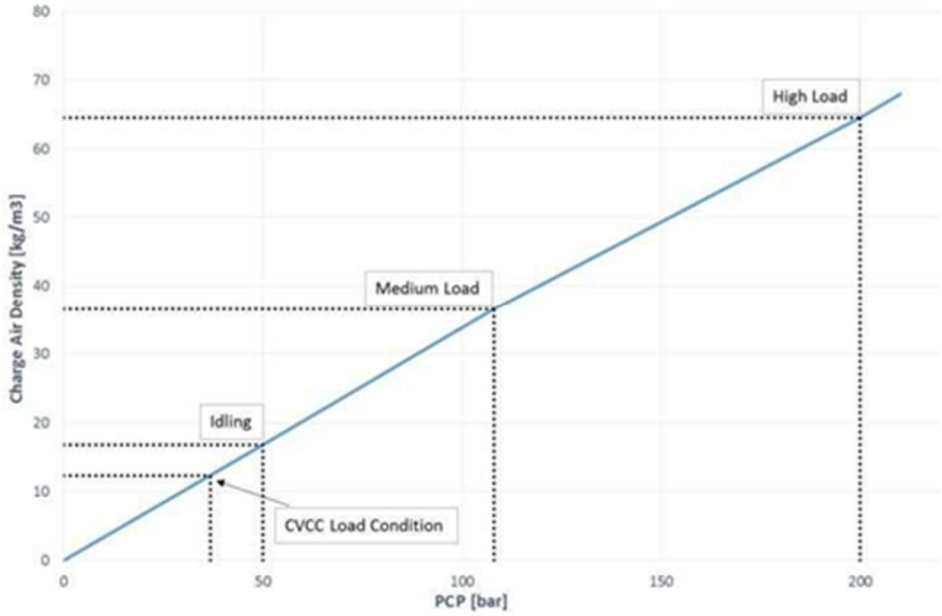

Figure 4.5 Typical load condition curve of medium speed CI engine in GT-Power simulation

4.4. Imaging technique

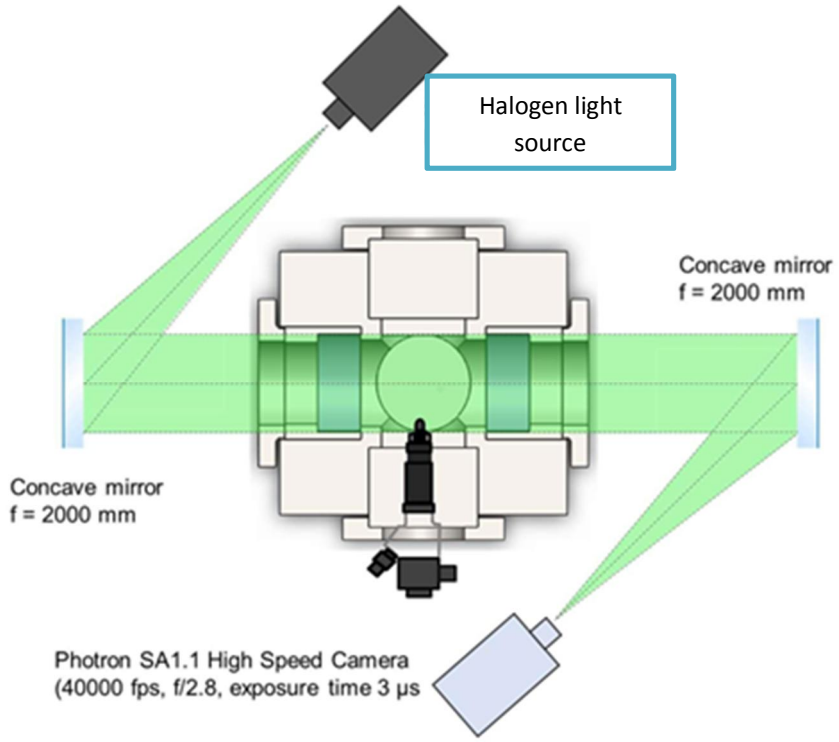

Figure 4.6 Z-type shadowgraph technique setup for image capture

During experiments, the environmental gas inside the chamber was changed into

nitrogen from air for the purpose of preventing autoignition or reactivity of the fuel at high ambient temperature. A halogen lamp was used as the light source. The vapor-phase spray images were taken by the shadowgraph method during the experiment. A Z-shaped arrangement was used in this experiment for higher test accuracy, which not only saved space, but also eliminated the phase difference caused by light reflection. The environmental gas during the experiment was also nitrogen. The shadowgraph method is an effective optical technique for displaying the vapor-phase spray. The background gas was compressed air during the experiment. All the camera parameter settings are shown in **Table 4.3**.

Table 4.3 Camera parameter

Frame rate (frames/sec)	30000
Exposure time (s)	1/500000
Image resolution	512x256 pixels

4.5. Test conditions

Diesel was blended with 20% by volume of the Ethanol and selected as the experimental fuel throughout the experiment. The physical and chemical properties of the fuel mixture are shown in **Table 4.4**.

Table 4.4 Physical and chemical properties of Diesel and Ethanol

Property	Fuel	
	Diesel	Ethanol (anhydrous)
Density at 15°C [kg/m^3]	820 - 845	792
Cetane number (CFR)	min. 51	~8
Lower Heating Value [MJ/kg]	43.700	26.900
Kinematic viscosity at 40°C [mm^2/s]	2 – 4.5	1.13
Flash point [°C]	min. 55	12.8
Autoignition temperature [°C]	~ 315	~ 423
C [wt. %]	~ 85.24	~ 52.17
H [wt. %]	~ 13.92	~ 13.04
O [wt. %]	~ 0.74	~ 34.78
S [wt. %]	max. 0.01	0.0
C/H mass ratio [-]	6.12	3.97
Stoichiometric Air/Fuel ratio [-]	14.60	9.01
Adiabatic flame temperature [°C] (determined from stoichiometric mixture at 9 MPa and 626 °C) [32]	2465	2401

In this experiment, the spray characteristics of the diesel/ethanol blends fuels under non-combustion evaporation conditions were visually measured respectively. The experimental conditions involved are shown in **Table 4.5**. A single hole injector with a 0.2 mm diameter

was applied in the experiment. The variations include the ambient pressure of 15 MPa and 30 MPa, the injection pressure from 500-1100 bar at 300 bar of step, and the injection duration of 800 μs to 1600 μs with the step of 400 μs.

Table 4.5 Experimental test matrix for DE20 blend

Fuel type	DE20
Injection Pressure (bar)	500-800-1100
Ambient gas density (kg/m^3)	15-30
Injector nozzle type	Single-hole
Injection duration (μs)	800-1200-1600
Ambient temperature (K)	293

Detailed macroscopic spray characteristics including spray penetration length, spray penetration rate, spray cone angle and spray area were investigated and analytically illustrated in the results and discussion section.

4.6. Image processing and macroscopic spray definitions

All the images of this experiment are processed by an in-house Matlab code. For the processing of liquid-phase spray images, the images are first converted to a grayscale images, then the color between the spray and the background is reversed, then the images are removed from the background, and noise reduction and brightness enhancement are performed to obtain the final desired images. While the background of shadowgraph is variegated and change rapidly due to thermal flow turbulence. Therefore, a different background removal method, consisting of subtracting between two adjacent images, was applied to process the data and obtain high-quality images.

The definition of macroscopic spray characteristics is shown in **Figure 4.7** and **Figure 4.8**, including spray penetration length, spray cone angle and projected spray area. Spray penetration is defined as the distance between the nozzle to the farthest axial location of spray boundary. The projected spray area is defined as the sum of the unit pixel areas within the spray boundary.

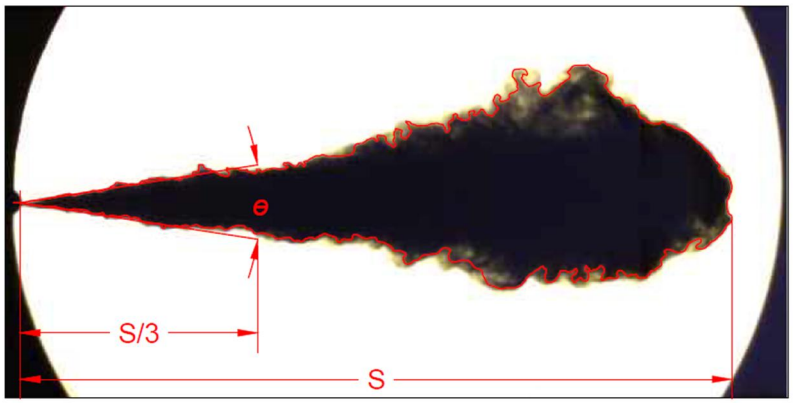

Figure 4.7 Spray penetration length and Spray cone angle definition

Figure 4.7 shows the boundary detected fuel spray according to the definition of Siebers and Naber [69]. To convert number of pixels into a measure of distance, number of pixels will first be collected from the PFV4 Program before multiplying with the scaling ratio between the image and the real dimension parameters to obtain approximate spray results.

The resulting spray cone angle is captured through spray imaging and then processed by MATLAB code to provide an accurate value and is suitable for data analysis with a remarkably large number of images.

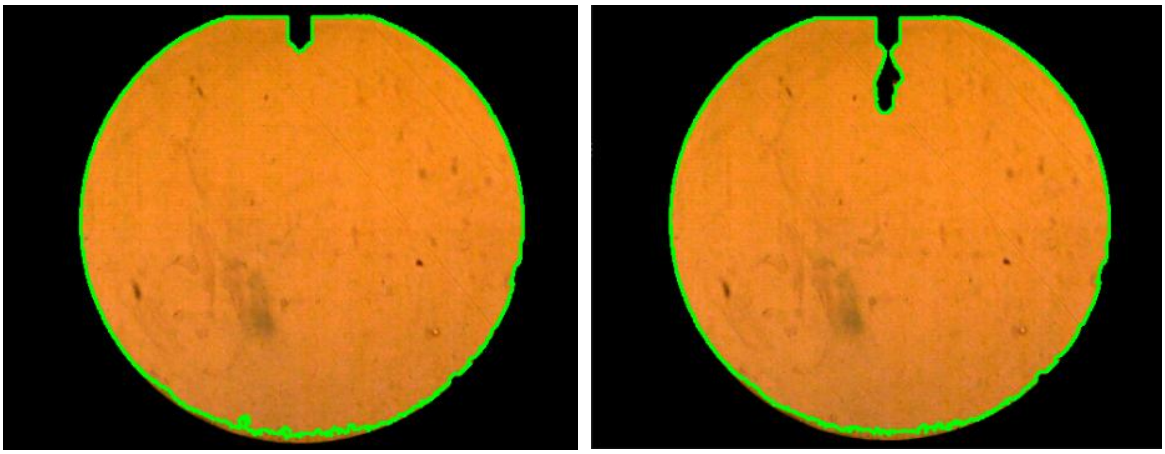

Figure 4.8 Spray area detection using subtracting method

In addition, spray area, which is detected by using the subtracting method, shown in **Figure 4.8**, by counting number of pixels between the first accounted image and the subsequential images. As the pixels to distance have been converted and a pixel is counted as a square, approximation of the 2D spray area can be assessed. During the spray formation process, turbulence within the spray is complex, so the assessment of the spray area is approximate. Nevertheless, it can represent a comparison between different test cases and therefore, highlighting the connection interaction with spray penetration and spray cone angle.

5. RESULTS AND DISCUSSIONS

5.1. Spray penetration length

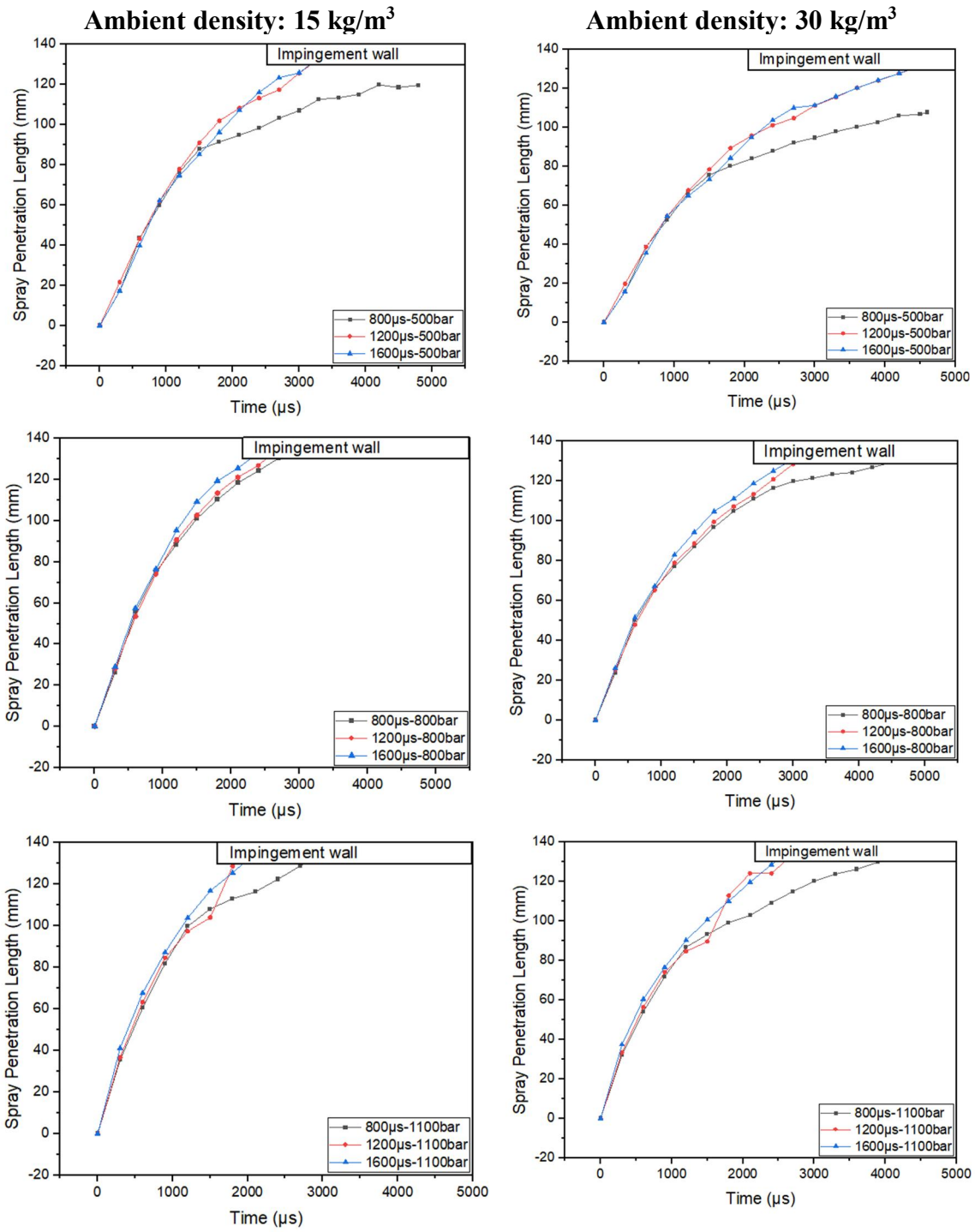

Figure 5.1 Spray penetration length of DE20 in comparison between ambient pressure of 15 MPa and 30 MPa, with varied injection duration from 800 µs to 1600 µs and injection pressure from 500 bar to 100 bar

The spray penetration length of DE20 fuel is shown in **Figure 5.1** with the experiment condition listed above. In this study, the injection duration is varied from 800 μs to 1600 μs with the step of 400 μs, the injection pressure is considered from 500 bar to 1100 bar with the step of 300 bar while the ambient pressure is separated into two columns with the left column considering 15 kg/m^3 and the right column considering 30 kg/m^3. The results are presented with a time step of 300 μs. Experimental comparisons are guaranteed to be under the same conditions of optical setup to avoid the influence of uncertainty. The permissible error in all test cases does not exceed 2% including auxiliary equipment. To determine the spray penetration length, the start and end points are decided by the position of the injector tip with the variable spray until impinged on the wall.

The spray tip penetration time is separated into two main areas by a key breakup time based on spray characteristics theories proposed. The spray breakup time (t_{break}) is based on the equations of Hiroyasu and Arai[70], which can be expressed as:

$$t_{break} = 28.65 \frac{\rho_f \, d_o}{\sqrt{\rho_c \Delta P}}$$

The details of the equation construction process have been presented in the previous study with relevant parameters. The results of the t_{break} moment are in line with the respective values of injection pressure and ambient gas density. T_{break} is defined as an intersection, when $t < t_{break}$ the spray development and remains in the primary breakup region, and the spray penetration length tends to be linear. During this stage, the spray droplets emerge from the nozzle hole with a large spray angle and pointed tip structure before breaking due to the fact that when $t > t_{break}$, the fuel from the injector continues to be molecularized into smaller droplets thanks to the resistance of the external pressure and the density of the liquid and gas. At this time, the fuel enters the secondary injection stage and the spray development is slow due to the influence of the surrounding gas density. The development of spray penetration length is nonlinear and distinct from that of the primary spray stage. In this present work, we also observed this two-stage based spray tip development phenomena.

Higher injection pressure results in increased spray penetration length, which can be attributed to increased spray momentum flux. This considerable rise is seen following the secondary breakup stage (t_{break}). However, the resulting spray penetration length has a longer penetration time with increasing ambient air density. Also, this study's lowest injection pressure case is 500 bar, which resulted in a complete absence of spray break before

impingement on the wall.

The injection pressure and spray duration are selected as the variation with the pressure varying from 500 bar to 1100 bar, while the spray duration is kept at 800 μs, 1200 μs, and 1600 μs respectively. Comparison between 2 cases of 15 kg/m^3 and 30 kg/m^3 of ambient pressure is then carried out. As a result of this, the results' trend is in line with the research from Chengjun Du [71]. Nevertheless, what makes the research different is the availability of longer observation time and longer injection pathway (Maximum length of 145 mm of visibility and 5000 μs), thereby allowing for detailed penetration length analysis.

Overall, it can be observed that with the case of 15 kg/m^3 ambient pressure, the fuel spray penetrated much faster than those test cases of 30 kg/m^3. Additionally, injection pressure can be seen to have the mandatory impact on the spray penetration length of the spray.

For the 15 kg/m^3 of ambient pressure, the spray injection with duration of 800 μs and 500 bar was not able to reach the impingement wall even after a very long period of nearly 5000 μs, while at longer injection duration, due to the mass momentum the spray tended to reach the wall at the same time for both 1200 μs and 1600 μs cases. Similar trend was observed for the case of increased ambient density until 30 kg/m^3. Nevertheless, at 500 bar of injection pressure inside the chamber's gas density of 15 kg/m^3, it took more than 3000 μs for injection duration of 1200 μs and 1600 μs to reach the wall while an addition of nearly 1300 μs for the similar cases but inside 30 kg/m^3 chamber's gas density to impinge on the wall. The penetration length difference for the 2 ambient densities at 800 μs of injection duration was witnessed at roughly 20 mm at non-impinging stage (1st row of the graph). At higher injection pressure of 800 bar, the spray development of the three cases of 800-1200-1600 μs rapidly rose in parallel to each other, with variations were minimal, depending mostly on the amount of fuel injection. However, at the lowest consideration of injection duration for the case of 30 kg/m^3 of ambient density, it takes 1800 μs more of time for the spray to reach the wall.

At the highest injection pressure under studying at 1100 bar, the spray penetration was dramatically rising at start of injection until 1200 μs, with another 800 μs starting to rise gradually. By contrast, higher injection duration allows for continuous rapid length raise. Higher ambient density also limited the development of the spray penetration length, especially limiting that of lower injection duration thoroughly all over the graphs.

Details of the spray development process can be observed when concerning the variations of the spray penetration rate of the consider tests cases of this study.

5.2. Spray penetration rate

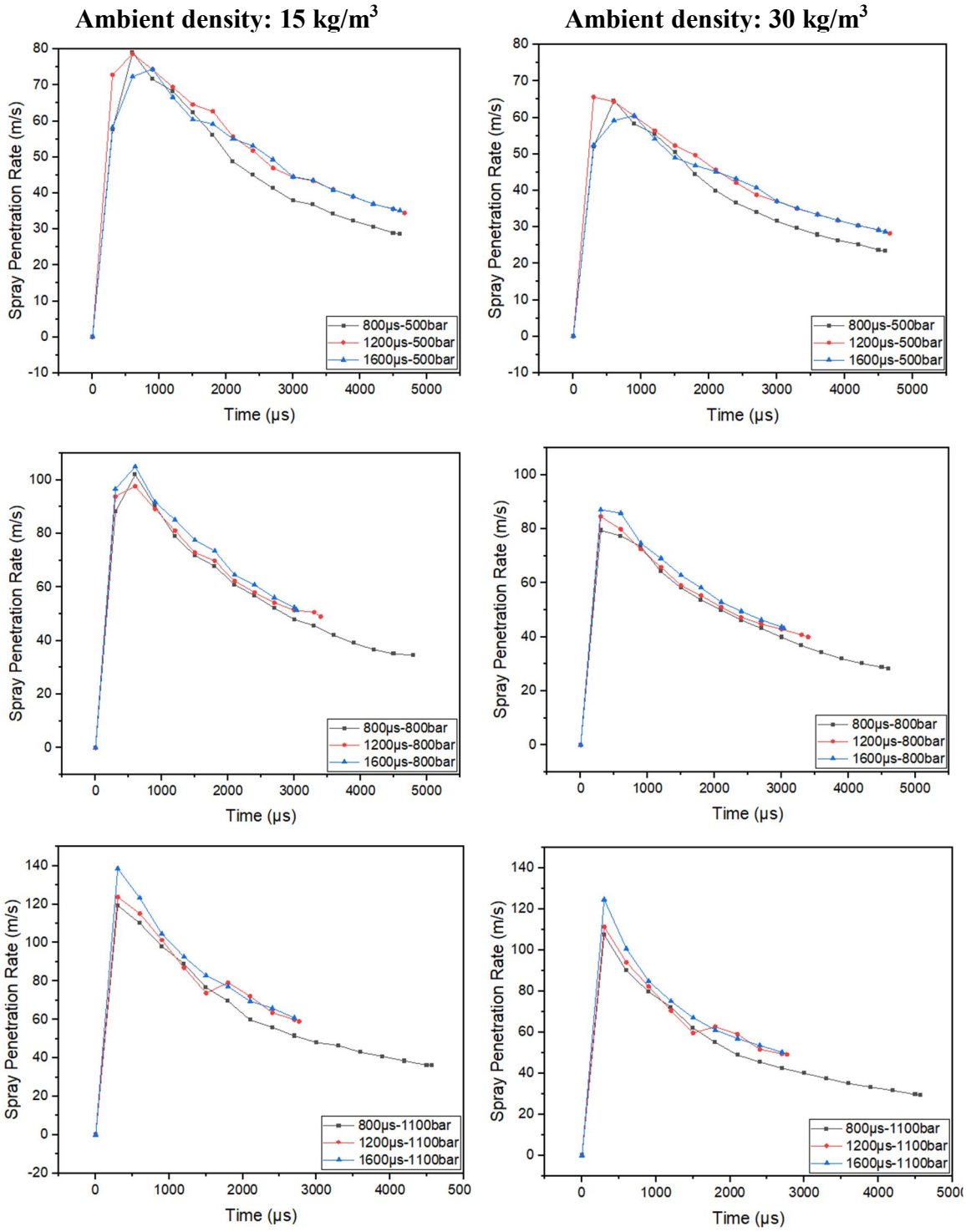

Figure 5.2 Spray penetration rate of DE20 in comparison between ambient pressure of 15 MPa and 30 MPa, with varied injection duration from 800 µs to 1600 µs and injection pressure from 500 bar to 100 bar

The spray penetration rate results are shown in **Figure 5.2** Although the spray penetration rate results are mainly based on the spray penetration length, it helps to show the specific development process in a clearer view. The spray penetration rate is calculated based on spray penetration length over time. As shown in the results, the spray penetration rate peaks at before 500 μs after it starts to appear and decreases over time until the spray impingement on the wall. The fluctuation in spray penetration rate over time can be explained by the fact that during the injection phase, the fuel injected in the previous stage undergoes acceleration due to the large pressure difference between the nozzle's inside and outside gas density. Then, because of the promotion of the amount of the fuel in the next phase, the volume of the spray beam increases along with the diffusion by temperature, and the surrounding environment hinders the axial force of the spray to make the velocity slow down and cause a strong deceleration. After the spray beam enters the steady state, it means that the fuel is continuously supplied, causing the kinetic energy of the spray beam to increase to achieve a balance between the main thrust of the spray beam and the drag force of the outside ambient density. At this point, the spray penetration rate is still decelerating but with a slower amplitude until impingement on the wall.

In summary, the injection pressure and ambient density have direct impacts on the rate of spray penetration, resulting in increased of both rating value and acceleration when the aforementioned factors are increased. Take an example of highest value recorded for the case of injection pressure of 500 bar and 1100 bar, the difference is calculated to be nearly 60 m/s, not to mentioned that when the ambient density is raised to 30 kg/m^3, at 500 bar of injection pressure, the variation is nearly 15 m/s. Even though the peak penetration rate varies greatly with increased injection pressure, variations in peak spray penetration rate between 2 ambient density cases are of similar difference at roughly around 15 m/s for the same injection pressure between the 2 cases. Lastly, the spray penetration rate slumping periods show a fluctuation in a downward trend, this can be explained by the intermittent characteristics of the injection scheme.

All test cases showed penetration rates within the allowable range and similar trends to related case studies previously done by the research group. The penetration rate peak values were recorded at 80, 105, and close to 140 m/s for the ambient density of 15 kg/m^3 while those of 30 kg/m^3 witnessed a peak at 70, 90, 130 m/s. In addition, it can be generalized from the graph that, although injection duration has had considerable influence on the spray penetration rate as well as the penetration length, at the lowest case study of 500 bar injection

pressure, peak value of penetration rate was recorded at 1200 μs of injection duration, followed by the 800 μs case, for both the cases of ambient density comparison. It can be considered that injection duration may have little impact on accelerating the rate of spray penetration at relatively low injection pressure.

5.3. Spray cone angle

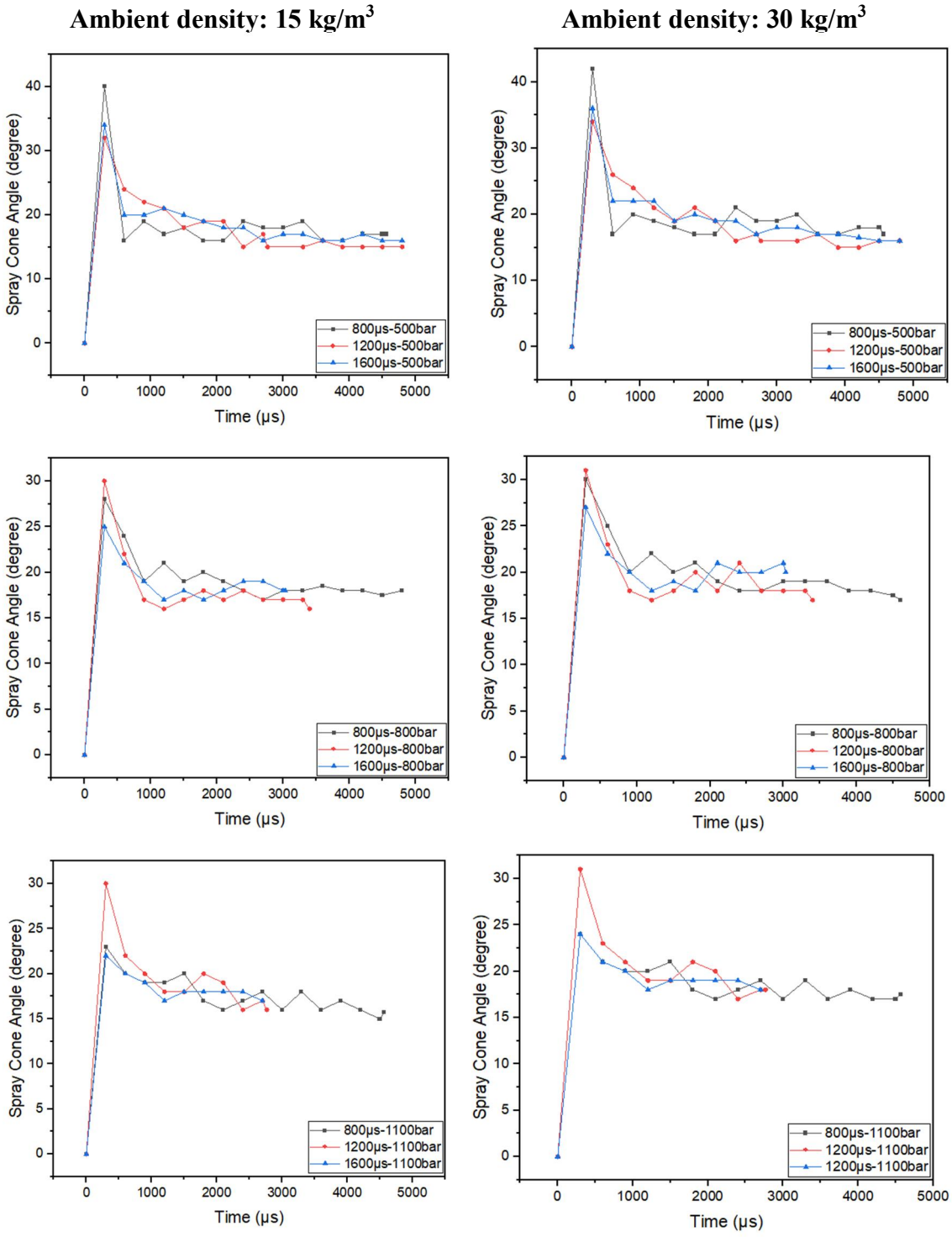

Figure 5.3 Spray cone angle of DE20 in comparison between ambient pressure of 15 MPa and 30 MPa, with varied injection duration from 800 µs to 1600 µs and injection pressure from 500 bar to 100 bar

Figure 5.3 illustrates the spray cone angle of DE20 with a blending between 20% ethanol and 80% diesel by volume at varied injection pressure from 500 to 1100 bar while increasing injection duration from 800 μs to 1600 μs and 2 ambient pressures of 15 kg/m^3 and 30 kg/m^3. The spray angle for all the test cases showed a sharp increase after the start of injection. This can be explained by the fact that the radial velocity of the liquid jet drastically changed, and the spray had a blob-like shape at the outset due to the injection needle valve opening and fuel flow inside the nozzle. Subsequently, the cone angle decreased rapidly under the influence of ambient gas. The effect of fuel type, however, cannot be clearly compared in such cases. With the evolution of the spray, the fuels gradually achieved a stable flow state after the needle valve was fully opened, and the spray cone angle approached a constant value. With the addition of the ethanol to diesel, which is in turn, reducing the viscosity and density of the DE20 fuel mixture, the liquid jet of the ternary blends was more likely to disintegrate into ligaments or droplets, as mentioned previously; and this contributed to the spray radial diffusion. In addition, the density of the blended fuel decreased with the add-up of considerably high percentage of ethanol, resulting in a smaller initial momentum, which reduced the ability of the spray to withstand the aerodynamic drag; therefore, the spray expanded in the radial direction. A larger spray cone angle contributes to better air entrainment into the spray, facilitating the uniformity of the fuel-air mix [72].

Besides, the average value of spray cone angle reduction is considered according to the development time of the spray. The maximum reduction at 500 bar of injection pressure is 59.5% while that of the 1100 bar case is only roughly about 43%. As proof of stable operation and spray formation as well as better supplement to the engine operating at high injection pressure, the blends showed a great potential of becoming among the competitors for renewable fuels.

5.4. Spray area

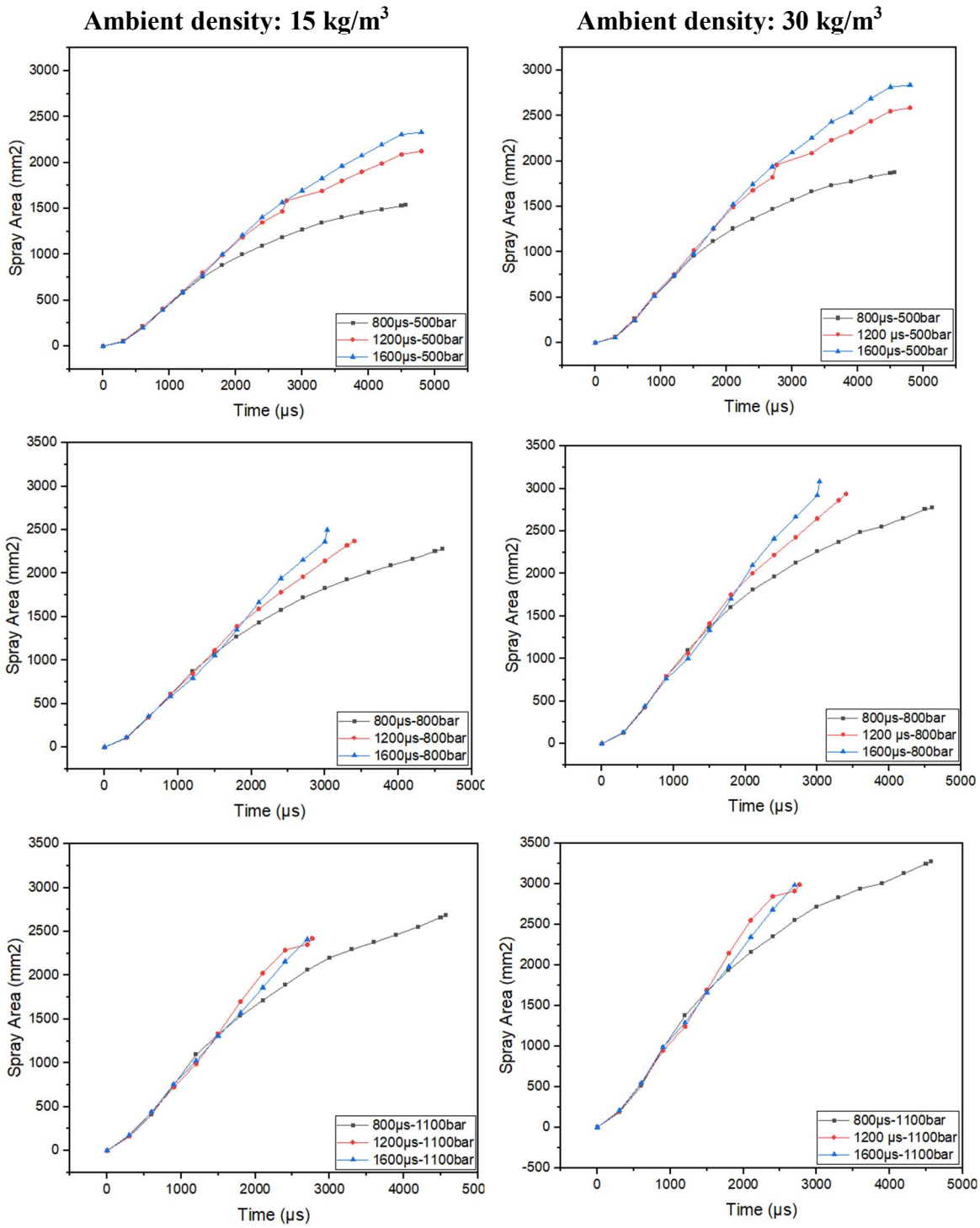

Figure 5.4 Spray area of DE20 in comparison between ambient pressure of 15 MPa and 30 MPa, with varied injection duration from 800 µs to 1600 µs and injection pressure from 500 bar to 100 bar

The spray area is an important parameter in the spray characteristics to evaluate the injection process. During the experiment, the spray area is calculated based only on the

change in pixel count of the next and first images of the process. The assessment of the spray area is only approximate because the results are only obtained as 2D images while the spray beam is formed in 3D space. During the spray formation process, turbulence within the spray is complex, so the assessment of the spray area is not entirely accurate, but it can represent a comparison between different test cases and can highlight the connection interaction with spray penetration and spray cone angle.

Figure 5.4 shows the trend of resulted spray area of DE20 under 2 ambient density of 15 kg/m^3 and 30 kg/m^3, with varied injection pressure from 500-1100 bar and injection duration at 800-1200-1600 μs. Generally, it can be seen observed from the graph that the higher injection pressure, regardless of the two ambient densities, the faster the growth value of the spray value. Secondly, increased injection duration notably promoted the projected spray area. For the most viable part lengthening the spray injection duration raised the spray area, however, for the case of highest under-considering injection pressure at 1100 bar, the injection duration of 1200 μs showed a higher value of spray area over the time, especially from after around 1500 μs until the spray reaches the wall. This can be explained by the outstanding value of the spray cone angle difference, making the area larger not only vertically but horizontally.

On top of that, another remarkable feature is that as the gas density increases, the spray area tends to follow the same pattern. A proper explanation to this instance is that when the gas density increases, it creates a great resistance and causes an imbalance in the spray forming process, making the spray to diffuse to the sides and gradually reduce the spray impingement time to reach the wall.

6. CONCLUSION

The results of evaluating the effects of injection duration and pressures regarding injection and chamber innate via spray characteristics analysis of the Diesel-Ethanol blend (DE20) can be summarized as follows:

- Lower ambient pressure resulted in faster spray penetration compared to higher ambient pressure. Injection pressure had a significant influence on spray penetration length, while the effect of ambient density was minimal until a certain time threshold. Higher injection pressures led to rapid and parallel spray development, with longer durations allowing for continuous and faster penetration.
- Injection pressure and ambient density directly impact the spray penetration rate. Increasing these factors leads to higher penetration rates and acceleration. Injection duration also influences the spray penetration rate, but at relatively low injection pressure, the impact of injection duration is minimal.
- Injection duration may have less effect on accelerating the rate of spray penetration at lower injection pressures. The observed spray penetration rates fall within the acceptable range and align with related case studies.
- The spray cone angle exhibited a sharp increase at the start of injection due to changes in radial velocity and the initial blob-like shape of the spray. Subsequently, the cone angle rapidly decreased under the influence of ambient gas.
- The addition of ethanol to diesel reduced the viscosity and density of the fuel mixture, leading to increased disintegration of the liquid jet into ligaments or droplets and radial diffusion of the spray. The lower density of the blended fuel resulted in reduced initial momentum and allowed the spray to expand radially. A larger spray cone angle facilitated better air entrainment into the spray and improved fuel-air mixing.
- Higher injection pressure leads to faster growth of the spray area, irrespective of ambient density. Increased injection duration significantly promotes the projected spray area.
- Increasing gas density follows a similar pattern in the spray area. The increase in gas density creates resistance and disrupts the spray forming process, causing the spray to diffuse to the sides and gradually reducing the spray impingement time on the wall.

Longer observation time and injection pathway in the study provided detailed insights into the spray development process, revealing the variations in spray penetration rates for the different test cases and emphasizing the importance of considering injection pressure and ambient pressure conditions in fuel spray analysis. The findings demonstrate stable operation, favorable spray formation, and highlight the potential of DE20 fuel blend as a renewable fuel option. The blend's ability to perform well at high injection pressures positions it as a promising competitor in the field of renewable fuels.

7. LIMITATIONS AND FUTURE WORKS

Limitations:

- The study laid the scope specifically only on high ratio blending of Diesel-Ethanol blends under non vaporizing conditions. However, as there happened to be some problems occurred during the experimental period, making the author not being able to run the same condition with base fuel to have a clearer comparison on the effects of Ethanol additions to the spray characteristics of the fuel blend.
- The study still lacks the fuel test on specific fuel blends. However, a more detailed fuel properties test and parameters will be conducted in further studies where the author will change the proportion of Ethanol within the Diesel-Ethanol blends.
- During the mixing phase of the fuel blends, the author also tried with different purity of Ethanol, however, only the purity of 99.9% of Ethanol showed no phase separation and guaranteed fuel stability.

Future works:

- Conduct similar experimental testing condition on base fuels before making comparison to the above-discussed study.
- Carry on with changing the fuel blending ratio to find the appropriate threshold of fuel blends, at the same time, creating a database for spray investigations of fuel mixtures, beneficial to the development of Deep Learning Algorithms.
- Investigate the impacts of Ethanol purity on the spray characteristics of the Diesel-Ethanol blends.
- One comprehensive theory is that: the larger the spray cone angle, the better the mixture, but that can also be prevented by too much fuel being attached to the cylinder walls. Therefore, diameters of the injector's tip should also be considered under investigation.

8. REFERENCE

[1] Bardi M, Bazyn T, Bruneaux G, Johnson J, Lee S-Y, Malbec LM, et al. Engine Combustion Network (Ecn): Characterization and Comparison of Boundary Conditions for Different Combustion Vessels. At Sprays 2012;22:777–806. doi:10.1615/AtomizSpr.2012006083.

[2] Bardi M, Payri R, Malbec LM, Bruneaux G, Pickett LM, Manin J, et al. Engine Combustion Network: Comparison of Spray Development, Vaporization, and Combustion in Different Combustion Vessels. At Sprays 2012;22:807–42. doi:10.1615/AtomizSpr.2013005837.

[3] Baert RSG, Frijters PJM, Somers B, Luijten CCM, Boer W De, de Boer W. Design and operation of a high pressure, high temperature cell for HD diesel spray diagnostics: guidelines and results. SAE Pap 2009-01-0649 2009;4970. doi:10.4271/2009-01-0649.

[4] Upatnieks A, Mueller CJ, Martin GC. The influence of charge-gas dilution and temperature on DI diesel combustion processes using a short-ignition-delay, oxygenated fuel. SAE Trans 2005;114:773–85. doi:10.4271/2005-01-2088.

[5] Espey C, E. DJ. Diesel engine combustion studies in a newly designes optical-access engin using high-speed visualization and 2-d laser imaging. Sae 1993;SAE-930971. doi:10.4271/930971.

[6] Sung C-J, Curran HJ. Using rapid compression machines for chemical kinetics studies. Prog Energy Combust Sci 2014;44:1–18. doi:10.1016/j.pecs.2014.04.001.

[7] Pastor JV, Payri R, Garcia-Oliver JM, Nerva J. Schlieren Measurements of the ECN-Spray A Penetration under Inert and Reacting Conditions. SAE Tech Pap 2012-01-0456 2012. doi:10.4271/2012-01-0456.

[8] Phan A. Development of a Rate of Injection Bench and Constant Volume Combustion Chamber for Diesel Spray Diagnostics. 2009.

[9] Pickett LM, Genzale CL, Bruneaux G, Malbec L-M, Hermant L, Christiansen C, et al. Comparison of Diesel Spray Combustion in Different High-Temperature, High-Pressure Facilities. SAE Int J Engines 2010;3:156–81. doi:10.4271/2010-01-2106.

[10] International energy Agency. World energy outlook 2011. Technical report, IEA, 2011. Cited on pages 2 and 3. n.d.

[11] Radulescu IG, Panait M, Voica C. BRICS Countries Challenge to the World Economy New Trends. Procedia Econ Financ 2014;8:605–13. doi:http://dx.doi.org/10.1016/S2212-5671(14)00135-X.

[12] BP. Energy outlook insights 2035. Technical report, British Petrol, 2014. Cited on page 3. n.d.

[13] Galle J, Demuynck J, Vancoillie J, Verhelst S. Spray Parameter Comparison between Diesel and Vegetable Oils for Non-Evaporating Conditions 2012. doi:10.4271/2012-01-0461.

[14] Milton BE. Thermodynamics, Combustion and Engines. London ; Melbourne: Chapman & Hall; 2005.

[15] Stone R. Introduction to Internal Combustion Engines. Macmillan Educ, 2nd edition; 1999.

[16] Dec JE. Advanced compression-ignition engines—understanding the in-cylinder processes. Proc Combust Inst 2009;32:2727–42. doi:http://doi.org/10.1016/j.proci.2008.08.008.

[17] Cheng AS, Upatnieks A, Mueller CJ. Investigation of the impact of biodiesel fuelling on NOx emissions using an optical direct injection diesel engine. Int J Engine Res 2006;7:297–318. doi:10.1243/14680874JER05005.

[18] Tree DR, Svensson KI. Soot processes in compression ignition engines. Prog Energy Combust Sci 2007;33:272–309. doi:http://doi.org/10.1016/j.pecs.2006.03.002.

[19] Kennedy IM. Models of soot formation and oxidation. Prog Energy Combust Sci 1997;23:95–132. doi:10.1016/S0360-1285(97)00007-5.

[20]. Brandão, L.F.P.; Suarez, P.A.Z. Study of Kinematic Viscosity, Volatility and Ignition Quality Properties of Butanol/Diesel Blends. Braz. J. Chem. Eng. 2018, 35, 1405–1414. [CrossRef]

[21]. Nithyanandan, K.; Zhang, J.; Li, Y.; Wu, H.; Lee, T.H.; Lin, Y.; Lee, C.-F.F. Improved

SI engine efficiency using Acetone–Butanol– Ethanol (ABE). Fuel 2019, 174, 333–343. [CrossRef]

[22]. Prasad, K.S.; Rao, S.S.; Raju, V. Effect of compression ratio and fuel injection pressure on the characteristics of a CI engine operating with butanol/diesel blends. Alex. Eng. J. 2021, 60, 1183–1197. [CrossRef]

[23]. Kuszewski, H. 'Experimental investigation of the effect of ambient gas temperature on the autoignition properties of ethanol– diesel fuel blends'. Fuel 2018, 214, 26–38. [CrossRef]

[24]. Lapuerta, M.; Ramos, Á.; Barba, J.; Fernández-Rodríguez, D. Cold- and warm-temperature emissions assessment of n-butanol blends in a Euro 6 vehicle. Appl. Energy 2018, 218, 173–183. [CrossRef]

[25]. Taghizadeh-Alisaraei, A.; Rezaei-Asl, A. The effect of added ethanol to diesel fuel on performance, vibration, combustion and knocking of a CI engine. Fuel 2016, 185, 718–733. [CrossRef]

[26]. Kuszewski, H.; Krzemin´ ski, A.; Ustrzycki, A. Wpływ zawodnienia alkoholu na pochodna¸ liczbe¸ cetanowa¸ mieszaniny oleju nape¸- dowego z etanolem oraz dodatkiem dodekanolu. In Monografia Systemy i ´ Srodki Transportu Samochodowego; Oficyna wydawnicza Politechniki Rzeszowskiej: Rzeszów, Poland, 2017.

[27]. Baczewski, K.; Kałdo´ nski, T. Paliwa do Silników o Zapłonie Samoczynnym; WKŁ: Warszawa, Poland, 2008; ISBN 978-83-206-1705-4.

[28]. Laza, T.; Bereczky, A. Basic fuel properties of rapeseed oil-higher alcohols blends. Fuel 2011, 90, 803–810. [CrossRef]

[29]. Hansen, A.C.; Zhang, Q.; Lyne, P.W. Ethanol–diesel fuel blends—A review. Bioresour. Technol. 2005, 96, 277–285. [CrossRef] [PubMed]

[30] U.S. Department of energy. Department of Energy 2015. http://www.eia.gov/ (accessed July 17, 2015).

[31] U.S. Energy Information Administration. International Energy Statistics 2012. http://www.eia.gov/ (accessed July 16, 2015).

[32] ePURE. European Renewable Ethanol 2015. http://www.epure.org/ (accessed July 17,

2015).

[33] EBTP-SABS. European Biofuels Technology Ptaform n.d. http://biofuelstp.eu/ (accessed July 17, 2015).

[34] ePURE. European Renewable Ethanol: State of the Industry Report 2014 2014:32. http://www.epure.org/sites/default/files/publication/140612-222-State-of-the-Industry-Report- 2014.pdf.

[35]. Lapuerta, M.; Armas, O.; Herreros, J.M. Emissions from a diesel–bioethanol blend in an automotive diesel engine. Fuel 2008, 87, 25–31. [CrossRef]

[36]. Kuszewski, H.; Jaworski, A.; Ustrzycki, A. Lubricity of ethanol–diesel blends—Study with the HFRR method. Fuel 2017, 208, 491–498. [CrossRef]

[37]. Li, D.-G.; Zhen, H.; Xingcai, L.; Wu-Gao, Z.; Jian-Guang, Y. Physico-chemical properties of ethanol–diesel blend fuel and its effect on performance and emissions of diesel engines. Renew. Energy 2005, 30, 967–976. [CrossRef]

[38]. Tutak, W.; Lukács, K.; Szwaja, S.; Bereczky, A. Alcohol–diesel fuel combustion in the compression ignition engine. Fuel 2015, 154, 196–206. [CrossRef]

[39]. Torres-Jimenez, E.; Jerman, M.S.; Gregorc, A.; Lisec, I.; Dorado, M.P.; Kegl, B. Physical and chemical properties of ethanol–diesel fuel blends. Fuel 2011, 90, 795–802. [CrossRef]

[40]. Gnanamoorthi, V.; Devaradjane, G. Effect of compression ratio on the performance, combustion and emission of DI diesel engine fueled with ethanol–Diesel blend. J. Energy Inst. 2015, 88, 19–26. [CrossRef]

[41]. Kuszewski, H.; Jaworski, A.; Ustrzycki, A.; Lejda, K.; Balawender, K.; Wo´s, P. Use of the constant volume combustion chamber to examine the properties of autoignition and derived cetane number of mixtures of diesel fuel and ethanol. Fuel 2017, 200, 564–575. [CrossRef]

[42] Hansen AC, Vosloo AP, Lyne PWL, Meiring P. Farmscale application of an ethanol–diesel blend. Agric Eng S Afr 1982;16:50–3.

[43] Meiring P, Hansen AC, Vosloo AP, Lyne PWL. High concentration ethanol-diesel blends

for compression-ignition engines. SAE Technical Paper; 1983.

[44] Hashimoto I, Nakashima H, Komiyama K, Maeda Y, Hamaguchi H, Endo M, et al. Diesel-ethanol fuel blends for heavy duty diesel engines-a study of performance and durability. SAE Technical paper; 1982.

[45] Hansen AC, Zhang Q, Lyne PWL. Ethanol-diesel fuel blends - A review. Bioresour Technol 2005;96:277–85. doi:10.1016/j.biortech.2004.04.007.

[46] Torres-Jimenez E, Jerman MS, Gregorc A, Lisec I, Dorado MP, Kegl B. Physical and chemical properties of ethanol-diesel fuel blends. Fuel 2011;90:795–802. doi:10.1016/j.fuel.2010.09.045.

[47] U.S. Department of energy. Department of Energy 2015. http://www.eia.gov/ (accessed July 17, 2015).

[48] Lapuerta M, Armas O, Herreros JM. Emissions from a diesel-bioethanol blend in an automotive diesel engine. Fuel 2008;87:25–31. doi:10.1016/j.fuel.2007.04.007.

[49] Gerdes KR, Suppes GJ. Miscibility of ethanol in diesel fuels. Ind Eng Chem Res 2001;40:949–56.

[50] Armas O, Mata C, Martinez-Martinez S. Effect of an ethanol-diesel blend on a common-rail injection system. Int J Engine Res 2012;13:417–28. doi:10.1177/1468087412438472.

[51] Letcher TM. Diesel blends for Diesel-engines. S Afr J Sci 1983;79:4–7.

[52] Letcher TM, BAUTZ SB, THOM VJ, MAMAGOBO T, LANGUAGE P. TERNARY LIQUID-LIQUID PHASE-DIAGRAMS FOR DIESEL FUEL BLENDS. 1. S Afr J Sci 1980;76:130–2.

[53] Meiring P, Allan RS, Lyne PWL. Ethanol-based multiple component fuels for diesel tractors. American Society of Agricultural Engineers; 1981.

[54] Marek N, Evanoff J. The use of ethanol blended diesel fuel in unmodified, compression ignition engines: an interim case study. Proc. air waste Manag. Assoc. 94th Annu. Conf. Exhib. Orlando, FL, 2001.

[55] Hansen AC, Hornbaker RH, Zhang Q, Lyne PWL. On-farm evaluation of diesel fuel oxygenated with ethanol. Am Soc Agric Eng Pap 2001.

[56] Heywood JB. Internal combustion engine fundamentals. vol. 930. Mcgraw-hill New York; 1988.

[57] Moses CA, Ryan TW, Likos WE. Experiments With Alcohol/Diesel Fuel Blends in Compression- Ignition Engines. VI Int. Symp. Alcohol Fuels Technol., Guaruja, Brazil: 1980, p. 5–8.

[58] Kim HN, Choi BC. Effect of ethanol-diesel blend fuels on emission and particle size distribution in a common-rail direct injection diesel engine with warm-up catalytic converter. Renew Energy 2008;33:2222–8. doi:10.1016/j.renene.2008.01.002.

[59] Kim H, Choi B. The effect of biodiesel and bioethanol blended diesel fuel on nanoparticles and exhaust emissions from CRDI diesel engine. Renew Energy 2010;35:157–63. doi:10.1016/j.renene.2009.04.008.

[60] He B-Q, Shuai S-J, Wang J-X, He H. The effect of ethanol blended diesel fuels on emissions from a diesel engine. Atmos Environ 2003;37:4965–71. doi:10.1016/j.atmosenv.2003.08.029.

[61] Ren Y, Huang Z-H, Jiang D-M, Li W, Liu B, Wang X-B. Effects of the addition of ethanol and cetane number improver on the combustion and emission characteristics of a compression ignition engine. Proc Inst Mech Eng Part D J Automob Eng 2008;222:1077–87. doi:10.1243/09544070JAUTO516.

[62] Dernotte J, Hespel C, Foucher F, Houillé S, Mounaïm-Rousselle C. Influence of physical fuel properties on the injection rate in a Diesel injector. Fuel 2012;96:153–60. doi:10.1016/j.fuel.2011.11.073.

[63] Lapuerta M, García-Contreras R, Agudelo JR. Lubricity of Ethanol-Biodiesel-Diesel Fuel Blends. Energy & Fuels 2010;24:1374–9. doi:10.1021/ef901082k.

[64] Ghobadian B, Rahimi H, Tavakkoli Hashjin T, Khatamifar M. Production of bioethanol and sunflower methyl ester and investigation of fuel blend properties. J Agric Sci Technol 2008;10:225–32.

[65] Rahimi H, Ghobadian B, Yusaf T, Najafi G, Khatamifar M. Diesterol: An environment-friendly IC engine fuel. Renew Energy 2009;34:335–42. doi:10.1016/j.renene.2008.04.031.

[66] Naber JD, Siebers DL. Effects of Gas Density and Vaporization on Penetration and

Dispersion of Diesel Sprays 1996. doi:10.4271/960034.

[67] Meiring P, Allan RS, Hansen AC, Lyne PWL. Tractor performance and durability with ethanoldiesel fuel. Trans ASAE [American Soc Agric Eng 1983.

[68] Hansen AC, Mendoza M, Zhang Q, Reid JF. Evaluation of oxydiesel as a fuel for direct-injection compression–ignition engines. Final Rep Illinois Dep Commer Community Aff Contract IDCCA 2000:96–32434.

[69] Armas O, Martínez-Martínez S, Mata C. Effect of an ethanol-biodiesel-diesel blend on a common rail injection system. Fuel Process Technol 2011;92:2145–53. doi:10.1016/j.fuproc.2011.06.010.

[70] Shinjo J, Umemura A. Simulation of liquid jet primary breakup: dynamics of ligament and droplet formation. Int J Multiph Flow 2010;36(7):513–32.

[71] C. Du, S. Andersson, and M. Andersson, "Two-dimensional measurements of soot in a turbulent diffusion diesel flame: the effects of injection pressure, nozzle orifice diameter, and gas density," *Combust. Sci. Technol.*, vol. 190, no. 9, pp. 1659–1688, 2018.

[72] Wang,C.,A.Sahu,C.Coratella,C.Xu,J.Saul,andH.Xu.2019."Spray characteristics of a gasoline-diesel blend(ULG75) using high-speed imaging techniques. " Fuel 239(Mar):677–692. https://doi.org/10.1016/j .fuel.2018.10.135.